AIMS Mathematics, 11(5): 13257–13286.
DOI: 10.3934/math.2026547
Received: 26 February 2026
Revised: 08 April 2026
Accepted: 22 April 2026
Published: 13 May 2026

http://www.aimspress.com/journal/Math

Research article

Dynamical analysis of a Tumor-Macrophages interaction model governed by the Caputo-Fabrizio derivatives

A. E. Matouk[1,*], Eman Ali Ahmed Ziada[2], Ausif Padder[3], Monica Botros[4,5] and Taher S. Hassan[6]

[1] Department of Mathematics, College of Science Al-Zulfi, Majmaah University, Al-Majmaah, 11952, Saudi Arabia
[2] Basic Science Department, Nile Higher Institute for Engineering and Technology, Mansoura 35511, Egypt
[3] Symbiosis Institute of Technology, Hyderabad Campus, Symbiosis International (Deemed University), Pune, India
[4] Basic Science Department, Faculty of Engineering, Delta University for Science and Technology, Gamasa 11152, Egypt
[5] Faculty of Artificial Intelligence, Delta University for Science and Technology, Gamasa, 11152, Egypt
[6] Department of Mathematics, Faculty of Science, University of Ha'il, Ha'il 2440, Saudi Arabia

* **Correspondence:** Email: ae.mohamed@mu.edu.sa.

Abstract: The Caputo-Fabrizio derivative is considered to be one of the most successful tools of fractional modeling since it has non singular nuclei, which make it a better candidate for modeling some interdisciplinary models that rely on memory effects and hereditary features such as the mathematical models in biology. In this study, tumor-macrophages interactions are modeled via the Caputo-Fabrizio derivatives. The uniqueness of the model's solutions is shown. A convergence analysis based on the Adomian decomposition method (ADM) is proved. The error analysis using the ADM is discussed. The Picard method is applied to the considered model. According to the stability theory of fractional-order systems governed by the Caputo-Fabrizio derivatives, the stability conditions of the tumor-free, the tumor-dominant, and the co-axial or the existence equilibrium points are discussed. Numerical simulations are carried out to show the rich complex dynamics in the model, including the existence of chaotic attractors.

Keywords: Tumor-Macrophages interaction model; Caputo-Fabrizio derivatives; Picard method; stability conditions; chaos
Mathematics Subject Classification: 26A33, 45J05, 65M70, 65R20

1. Introduction

The mathematical models showing the interactions between tumors and the immune system exhibit complex dynamics due to their complex mathematical structures that contain many nonlinear terms. In fact, macrophages have an essential effect in controlling and promoting tumor growth. On the other hand, cancer is one of the causes of malignant tumors. In 2022, The International Agency for Cancer Research reported that nearly 9.7 million people worldwide died from cancer. Consequently, tumor reduction has become a focal topic of research interest. Recently, many systems on tumor-macrophage interactions have been modeled via integer-order differential equations [1, 2].

Recently, fractional calculus has received a lot of attention from researchers due to its multiple applications in various branches of science, economics, and technology [3–11]. Fractional-order derivatives are divided into several types depending on the kernel. The Caputo fractional derivative that is used in many applications is characterized by the singular kernel [12], while the Caputo-Fabrizio (CF) fractional derivative is characterized by the non-singular kernel [13]. Both of them are considered non-local operators because they are defined by integration. The Caputo-Fabrizio type has influential applications in many interdisciplinary fields such as signal processing [14], circuit design [15, 16], and DC-DC converter circuits [17].

In addition, the CF derivative is commonly used in many systems of mathematical biology that rely on the effects of memory and hereditary features such as cancer models [18], brain models [19], vector-host disease models [20], hepatitis E models [21], HIV models [22], human liver models [23], Brucellosis models [24], coronavirus models with comorbidity [25], vector-borne disease models [26], SIR models [27], susceptible-vaccinated-infected-recovered (SVIR) models [28], fuzzy Bidirectional associative memory (BAM) neural networks [29], and multidrug resistance models [30].

The fractional-order derivatives have shown great efficiency in describing biological systems, including tumor models, as they contain the memory effect and the hereditary properties necessary to describe these models with great accuracy. Recently, some tumor models have been studied that are based on fractional-order derivatives such as cancer models [31] tumor-immune models [32].

It has been proven that the Adomian decomposition method (ADM) is an effective analytical and numerical approach to resolving differential equations that commonly arise in the modeling of real-world physical phenomena. Originally developed by George Adomian during the 1970s through the 1990s, while he was serving as Chairman of Applied Mathematics at the University of Georgia, the method is distinguished by its utilization of Adomian polynomials. These polynomials ensure the convergence of the resulting series solution without requiring linearization or discretization of the nonlinear terms. Constructed as a Maclaurin series expansion with respect to an auxiliary parameter, Adomian polynomials provide a more flexible framework compared with traditional Taylor series expansions. Unlike conventional numerical techniques, the ADM yields closed-form solutions that depend solely on the initial conditions. Its advantages over techniques such as the Taylor series method, the homotopy perturbation method, and the Picard method (PM) are discussed in [33–35].

The ADM has demonstrated strong effectiveness and is applicable to the solution of nonlinear fractional differential equations [36–38], an area that continues to present promising directions for future scientific and technological studies. A key merit of the method is its universality, as it can be directly used to address a wide spectrum of differential equations, either linear or nonlinear, homogeneous or inhomogeneous, and with either constant or variable coefficients. Furthermore, the

ADM circumvents the need for linearization, discretizations, or the introduction of perturbation parameters when handling nonlinear terms. From a computational perspective, the method is efficient and practical, significantly reducing computational effort while preserving the high precision of the solutions obtained [39, 40].

The proposed fractional-order formulation, which includes the effects of previous states into the current dynamics, presents a more realistic framework for analyzing tumor-macrophage interactions as opposed to standard integer-order models. The fractional model reflects the inherited characteristics present in intricate biological processes by taking into consideration the impact of previous states, in contrast to integer-order systems that focus only on the current state. This characteristic is particularly essential for simulating tumor development and immunological responses, when history-dependent dynamics are vital. Likewise, the ADM, which uses Adomian polynomials to handle nonlinear variables in such nonlinear fractional systems, is very successful in producing quick convergent analytical series solutions without the need for linearization or discretization. As a result, the fractional-order formulation and the ADM combined to improve the problem's analytical modeling capability. It is especially useful for examining the qualitative characteristics of a system, since it maintains the analytical structure of the solution.

2. Mathematical background

The definition of the CF derivative of order ξ is [13]

$$ {}^{Cf}D_a^{\xi}\mathfrak{H}(t) = \frac{B(\xi)}{1-\xi}\int_a^t \exp\left(\frac{-\xi(t-s)}{1-\xi}\right)\mathfrak{H}'(s)ds, \tag{2.1} $$

while the normalization function $B(\xi) > 0$ satisfies $B(0) = B(1) = 1$. Its corresponding fractional integral is

$$ {}^{Cf}I_a^{\xi}\mathfrak{H}(t) = \frac{1-\xi}{B(\xi)}\mathfrak{H}(t) + \frac{\xi}{B(\xi)}\int_a^t \mathfrak{H}(s)ds, \quad \xi \in (0,1), \tag{2.2} $$

where

$$ \left({}^{Cf}I_a^{\xi}\right)\left({}^{CF}D_a^{\xi}\right)\mathfrak{H}(t) = \mathfrak{H}(t) - \mathfrak{H}(a). \tag{2.3} $$

This definition's primary benefit is that it does not contain any singularities.

The CF derivative satisfies the following properties.

Consider the CF operator ${}^{Cf}D_a^{\xi}$, $0 < \xi < 1$, and $a \le t \le T$. So, the CF operator satisfies the following properties [41, 42].

(1) The operator ${}^{Cf}D_a^{\xi}$ is linear, i.e.,

$$ {}^{Cf}D_a^{\xi}(s_1u + s_2v) = s_1{}^{Cf}D_a^{\xi}u + s_2{}^{Cf}D_a^{\xi}v, $$

for every $u, v \in D([a,T])$, where $D([a,T])$ represents the space of test functions, s_1 and s_2 are constants.

(2) The operator ${}^{Cf}D_a^{\xi}$, is bounded, which satisfies the inequality

$$ \left\|{}^{Cf}D_a^{\xi}u\right\|_{C^1([a,T])} \le \frac{\left(1-\exp(\frac{(T-a)\xi}{\xi-1})\right)}{\xi}\|u\|_{C^1([a,T])}. $$

(3) The operator ${}^{Cf}D_a^{\xi}$, is a distribution (continuous), i.e.

$$\left|{}^{Cf}D_a^{\xi}u - {}^{Cf}D_a^{\xi}u_n\right| \to 0,$$

for every $u, u_n \in D([a,T])$ given that u_n approaches u.

(4) The operator ${}^{Cf}D_a^{\xi}u(t) \in C^1([a,T])$ when $u \in C^1([a,T])$.

(5) Let $u \in C^m([a,T),\ m = 1,2,3,\ldots$. So, the mth derivative of the CF operator is given by

$$\frac{d^m}{dt^m}\,{}^{Cf}D_a^{\xi}u(t) = (-1)^m\left(\frac{\xi}{1-\xi}\right)^m\,{}^{Cf}D_a^{\xi}u(t) + \sum_{i=1}^{m}(-1)^{m-i}\frac{\xi^{m-i}}{(1-\xi)^{m-i+1}}u^{(i)}(t).$$

3. Description of the tumor-macrophages interaction model

In the following, the model is formulated via the CF fractional derivatives. First, we refer to the following model [43]:

$$\begin{aligned}
\frac{dT(t)}{dt} &= aT - abT^2 - fTM_1 + gTM_2,\\
\frac{dM_1(t)}{dt} &= e_1TM_1 - (r_1+d_1)M_1 + r_2M_2,\\
\frac{dM_2(t)}{dt} &= e_2TM_2 - d_2M_2 + r_1M_1 - r_2M_2,
\end{aligned} \tag{3.1}$$

where T represents the tumor cell populations, M_1 represents the anti-tumor macrophage populations and M_2 represents the pro-tumor macrophages populations. The other model's parameters are explained in [43]. A single feedback control strategy $F(t)$ is included in System (3.1) as the fourth variable to control the growth of T-cells with control rate μ_1. The strengths of $F(t)$ impact on M_1-cells and M_2-cells are represented by μ_2 and μ_3, respectively. The concentration level of $F(t)$ required in the body or available at time t is denoted by μ_4 the (reduction rate of F) and μ_5 (the concentration of F required in the presence of T-Cells). Thus, the tumor-macrophages interaction model governed by the Caputo-Fabrizio fractional derivatives is represented as

$$\begin{aligned}
{}^{Cf}D_0^{\xi}T(t) &= \alpha_1T(t)(1-\beta_1T(t)) - \gamma_1T(t)M_1(t) + \delta_1T(t)M_2(t) - \mu_1T(t)F(t),\\
{}^{Cf}D_0^{\xi}M_1(t) &= \alpha_2T(t)M_1(t) - (\beta_2+\gamma_2)M_1(t) + \delta_2M_2(t) - \mu_2M_1(t)F(t),\\
{}^{Cf}D_0^{\xi}M_2(t) &= \alpha_3T(t)M_2(t) - (\beta_3+\delta_2)M_2(t) + \gamma_2M_1(t) - \mu_3M_2(t)F(t),\\
{}^{Cf}D_0^{\xi}F(t) &= \mu_5T(t) - \mu_4F(t),
\end{aligned} \tag{3.2}$$

where ξ is the fractional-order with initial conditions $T(0) = 1$, $M_1(0) = 1$, $M_2(0) = 1$, and $F(0) = 1$.

The biological meaning of the previous system's parameters is explained in Table 1.

Table 1. The biological explanation and numerical values for each parameter in the model and their meanings.

Symbol	Value	Units	Description
$T(t)$	-	Cells	Size of the tumor at time t
$M_1(t)$	-	Arbitrary units	Level of anti-tumor macrophages at time t
$M_2(t)$	-	Arbitrary units	Level of pro-tumor macrophages at time t
$F(t)$	-	Arbitrary units	Level of feedback control at time t
γ_1	2×10^{-6}	1/day	T cells' death rate caused by M_1 cells
γ_2	0.05	1/day	M_1 cells' re-polarization rate to M_2 cells' rate
β_1	0.5×10^{9}	Cells	Maximum carrying capacity for the environment
β_2	0.2	1/day	M_1 cells' natural death rate
β_3	0.2	1/day	M_2 cells' natural death rate
δ_1	10^{-7}	1/day	T cells' proliferation rate when M_2 cells are found
δ_2	0.04	1/day	M_2 cells' rate of repolarization to M_1 cells
α_1	0.565	1/day	The tumor's growth rate
α_2	10^{-6}	1/day	M_1 cells' activation rate when T cells are involved
α_3	9×10^{-7}	1/day	M_2 cells' activation rate when T cells are involved
μ_1	1	1/day	Effect of F on T cells
μ_2	0.5	1/day	Effect of F on M_1 cells
μ_3	0.002	1/day	Effect of F on M_2 cells
μ_4	0.05	1/day	Rate of natural deterioration or decrease in F
μ_5	0.1	Cells	F concentration needed when T cells are included

The dimension of CF derivative in the previous system is of the form $t^{-\xi}$. So, all parameters in the above-mentioned model have exponents of the memory parameter ξ, which imply that they have dimensions of $t^{-\xi}$. Then, all the variables and parameters in Table 1 are rescaled to have dimensions of $1/t$. The resulting system is described as follows:

$$\begin{aligned} {}^{Cf}D_0^{\xi}w &= \alpha_1 w - \alpha_1\beta_1 w^2 + \delta_1 wy - \gamma_1 wx - \mu_1 wz, \\ {}^{Cf}D_0^{\xi}x &= -(\gamma_2+\beta_2)x + \delta_2 y + \alpha_2 wx - \mu_2 xz, \\ {}^{Cf}D_0^{\xi}y &= \gamma_2 x - (\delta_2+\beta_3)y - \mu_3 yz + \alpha_3 wy, \\ {}^{Cf}D_0^{\xi}z &= \mu_5 w - \mu_4 z, \end{aligned} \tag{3.3}$$

where x, y, z, and w denote the rescaled variables representing the variables of anti-tumor cells, pro-tumor cells, feedback control, and tumor cells, respectively. Now, each one of these variables has dimensions of $1/t$ and all the parameters have dimensions of $1/t$. In addition, the memory parameter ξ shows the effect of prior experiences on the dynamics of the model's populations, which makes the previous fractional models a better candidate for describing the behaviors of the considered tumor model.

System (3.3) has the following types of equilibrium states: Tumor-free equilibrium (TFE) (0,0,0,0), the tumor-dominant equilibrium (TDE) $\left(\frac{\mu_4\alpha_1}{\mu_1\mu_5+\mu_4\alpha_1\beta_1}, 0, 0, \frac{\mu_5\alpha_1}{\mu_1\mu_5+\mu_4\alpha_1\beta_1}\right)$, the co-axial or co-existence equilibrium points $(T_+, M_1^*, M_2^*, \frac{\mu_4}{\mu_5}T_+)$ and $(T_-, M_1^*, M_2^*, \frac{\mu_4}{\mu_5}T_-)$, where $T_{\pm}$ represents the

real roots of the equation:

$$T^2 - \mu_4\left(\frac{\delta_2+\beta_2}{\alpha_3\mu_4-\mu_3\mu_5}+\frac{\gamma_2+\beta_2}{\alpha_2\mu_4-\mu_2\mu_5}\right)T+\mu_4^2\left(\frac{\beta_2(\gamma_2+\beta_2)+\beta_2^2}{(\alpha_2\mu_4-\mu_2\mu_5)(\alpha_3\mu_4-\mu_3\mu_5)}\right)=0,$$

and

$$\begin{aligned} M_1^* &= -(\alpha_3 T-\delta_2-\beta_3-\frac{\mu_3\mu_5}{\mu_4}TM_2^*, \\ M_2^* &= \frac{\left[\frac{\mu_1\mu_5}{\mu_4 T}-\alpha_1(1-\beta_1 T)\right]\gamma_2}{\left(\alpha_3 T-\delta_2-\beta_3-\frac{\mu_3\mu_5}{\mu_4 T}\right)\gamma_1-\delta_1\gamma_2}. \end{aligned}$$

3.1. The equilibrium points' stability

The TFE has the following characteristic equation:

$$(\lambda+\mu_4)(\lambda-\alpha_1)(\lambda^2+\sigma_1\lambda+\sigma_2)=0,$$

where

$$\sigma_1=(\beta_2+\gamma_2+\delta_2+\beta_3) \text{ and } \sigma_2=-\delta_2\gamma_2.$$

Thus, according to [44], we obtain the following lemma.

Lemma 1. *If $\alpha_1<\frac{1}{1-\xi}$, the TFE is unstable. However, if $\alpha_1>\frac{1}{1-\xi}$, the following statements hold:*

(1) The TFE is locally asymptotically stable (LAS) for $\sigma_1>0$ and $\sigma_1^2<4\sigma_2$.

(2) The TFE is unstable for $\sigma_1<0,\ \sigma_2\in(0,1)$ and $\sigma_1^2<4\sigma_2$.

(3) The TFE is unstable for $\sigma_1<0,\ \left|\frac{-\sigma_1\pm\sqrt{\sigma_1^2-4\sigma_2}}{2}\right|<\frac{1}{1-\xi}$, and $\sigma_1^2<4\sigma_2$.

(4) The TFE is LAS for $\sigma_1>0,\ \sigma_2>0$, and $\sigma_1^2>4\sigma_2$.

(5) The TFE is LAS for $\sigma_2<0,\ \left|\frac{-\sigma_1+\sqrt{\sigma_1^2-4\sigma_2}}{2}\right|>\frac{1}{1-\xi}$, and $\sigma_1^2>4\sigma_2$.

(6) The TFE is unstable for $\sigma_2<0,\ \left|\frac{-\sigma_1+\sqrt{\sigma_1^2-4\sigma_2}}{2}\right|<\frac{1}{1-\xi}$, and $\sigma_1^2>4\sigma_2$.

The TDE has the following characteristic equation:

$$(\lambda-c_1)(\lambda-b_1)(\lambda^2+\acute{\sigma}_1\lambda+\acute{\sigma}_2)=0,$$

where

$$\begin{aligned} a_1 &= \alpha_1-\mu_1\acute{F}-2\alpha_1\beta_1\acute{T},\ b_1=\alpha_2\acute{T}-\mu_2\acute{F}-\gamma_2-\beta_2,\ c_1=\alpha_3\acute{T}-\mu_3\acute{F}-\delta_2-\beta_3, \\ \acute{\sigma}_1 &= \mu_4-a_1,\ \acute{\sigma}_2=\mu_1\mu_5\acute{T}-\mu_4 a_1,\ \acute{T}=\frac{\mu_4\alpha_1}{\mu_1\mu_5+\mu_4\alpha_1\beta_1} \text{ and } \acute{F}=\frac{\mu_5\alpha_1}{\mu_1\mu_5+\mu_4\alpha_1\beta_1}. \end{aligned}$$

Obviously, Lemma 1 indicates that tumors might not be entirely removed naturally without assistance if condition (2), (3), or (6) holds. However, the T-cells overcome immunosuppression and tumor growth if condition (1), (4), or (5) holds.

According to [42, 44], the following lemma is derived.

Lemma 2. *If* $0 < c_1 < \frac{1}{1-\xi}$ *or* $0 < b_1 < \frac{1}{1-\xi}$, *the TDE is unstable. However, if* $\min(c_1, b_1) > \frac{1}{1-\xi}$, *the following statements hold:*

(1) The TDE is LAS for $\acute{\sigma}_1 > 0$ *and* $\acute{\sigma}_1^2 < 4\acute{\sigma}_2$.

(2) The TDE is unstable for $\acute{\sigma}_1 < 0,\ \acute{\sigma}_2 \in (0, 1)$ *and* $\acute{\sigma}_1^2 < 4\acute{\sigma}_2$.

(3) The TDE is unstable for $\acute{\sigma}_1 < 0,\ \left|\frac{-\acute{\sigma}_1 \pm \sqrt{\acute{\sigma}_1^2 - 4\acute{\sigma}_2}}{2}\right| < \frac{1}{1-\xi}$, *and* $\acute{\sigma}_1^2 < 4\acute{\sigma}_2$.

(4) The TDE is LAS for $\acute{\sigma}_1 > 0,\ \acute{\sigma}_2 > 0$, *and* $\acute{\sigma}_1^2 > 4\acute{\sigma}_2$.

(5) The TDE is LAS for $\acute{\sigma}_2 < 0,\ \left|\frac{-\acute{\sigma}_1 + \sqrt{\acute{\sigma}_1^2 - 4\acute{\sigma}_2}}{2}\right| > \frac{1}{1-\xi}$, *and* $\acute{\sigma}_1^2 > 4\acute{\sigma}_2$.

(6) The TDE is unstable for $\acute{\sigma}_2 < 0,\ \left|\frac{-\acute{\sigma}_1 + \sqrt{\acute{\sigma}_1^2 - 4\acute{\sigma}_2}}{2}\right| < \frac{1}{1-\xi}$, *and* $\acute{\sigma}_1^2 > 4\acute{\sigma}_2$.

The co-existence or interior equilibrium point say $(T^*,\ M_1^*,\ M_2^*,\ F^*)$ has the following characteristic polynomial equation:

$$P(\lambda) = \lambda^4 + \eta_1\lambda^3 + \eta_2\lambda^2 + \eta_3\lambda + \eta_4 = 0,$$

where

$$\begin{aligned}
\eta_1 &= \mu_5 + \mu_4 - \varpi_4,\ \eta_2 = \varpi_5 - \mu_5\varpi_1 - \mu_4\varpi_4,\ \eta_3 = \mu_5\varpi_2 + \mu_4\varpi_5 - \varpi_6,\ \eta_4 = -\mu_5\varpi_3 - \mu_4\varpi_6,\\
\varpi_1 &= \delta_2 - \gamma_1 T^* - \mu_3 M_2^*,\\
\varpi_2 &= \mu_2 c_2 M_1^* - \mu_3\delta_2 M_2^* + \mu_3\gamma_1 T^* M_2^* + \mu_1\gamma_2 T^* - \delta_2\gamma_1 T^* - \delta_1 b_2 T^*,\\
\varpi_3 &= -\mu_1 T^*(c_2 b_2 - \delta_2\gamma_2) - \gamma_1 T^*(\mu_2 c_2 M_1^* - \mu_3\delta_2 M_2^*) - \delta_1 T^*(\mu_2\gamma_2 M_1^* - \mu_3 b_2 M_2^*),\\
\varpi_4 &= c_2 + b_2 + a_2,\\
\varpi_5 &= c_2(a_2 + b_2) + a_2 b_2 - \delta_2\gamma_2 - \alpha_3\delta_1 T^* M_2^* + \alpha_2\gamma_1 T^* M_1^*,\\
\varpi_6 &= a_2(c_2 b_2 - \delta_2\gamma_2) + \delta_1 T^*(\alpha_2\gamma_2 M_1^* - \alpha_3 b_2 M_2^*) + \gamma_1 T^*(\alpha_2 c_2 M_1^* - \alpha_3\delta_2 M_2^*),\\
a_2 &= \alpha_1 - \mu_1 F^* - 2\alpha_1\beta_1 T^* + \delta_1 M_2^* - \gamma_1 M_1^*,\\
b_2 &= \alpha_2 T^* - \mu_2 F^* - \gamma_2 - \beta_2, \text{ and } c_2 = \alpha_3 T^* - \mu_3 F^* - \delta_2 - \beta_3.
\end{aligned}$$

Obviously, Lemma 2 implies the existence of immune-mediated latency or tumor dormancy if Condition (1), (4), or (5) holds, where the immune system controls the tumor, preventing its further growth, even if complete eradication is not achieved. This means that the immune system might not always be enough to inhibit tumor growth permanently. However, the other conditions mean that the immune response is strong, leading to tumor elimination.

According to [44], the following lemma is derived.

Lemma 3. *The co-existence or interior equilibrium state* $(T^*,\ M_1^*,\ M_2^*,\ F^*)$ *fulfills the following conditions:*

(i) The equilibrium state $(T^*,\ M_1^*,\ M_2^*,\ F^*)$ *is LAS when the discriminant* $D(P(\lambda)) < 0,\ \frac{\eta_3}{\eta_1\eta_2} = 1 - \frac{\eta_1\eta_4}{\eta_2\eta_3}$, *where* $\eta_i > 0 \forall i = 1, 2, 3, 4$.

(ii) The equilibrium state $(T^*,\ M_1^*,\ M_2^*,\ F^*)$ *is LAS if* $\eta_3^2 + \eta_4\eta_1^2 - \eta_1\eta_2\eta_3 = 0$ *and* $\eta_1\eta_2 - \eta_3 > 0$, *where* $\eta_4 > 0$ *and* $\eta_1 > 0$.

(iii) The equilibrium state $(T^*,\ M_1^*,\ M_2^*,\ F^*)$ *is unstable if* $D(P(\lambda)) < 0,\ \eta_2 > 0,\ \eta_3 < 0,\ \eta_4 > 0$, *and* $\frac{1}{1-\xi} > \rho^2$, *where* $\rho = \max(-\eta_4, -\eta_3, -\eta_2, -\eta_1) + 1$.

(iv) The equilibrium state $(T^*,\ M_1^*,\ M_2^*,\ F^*)$ *is LAS if either* $(P(0)P(l_1) < 0$ *and* $l_2 < 0)$ *or* $(P(\frac{1}{1-\xi})P(l_2) < 0$ *and* $l_1 > \frac{1}{1-\xi})$ *, where* $D(P(\lambda)) > 0$*,* $l_1 = -\frac{\eta_1}{4} - \frac{3}{4}\sqrt{\eta_1^2 - \frac{8}{3}\eta_2}$ *, and* $l_2 = -\frac{\eta_1}{4} + \frac{3}{4}\sqrt{\eta_1^2 - \frac{8}{3}\eta_2}$.

Obviously, Lemma 3 indicates that tumor suppression may be possible under particular control settings and immune activation, as indicated by Conditions (i), (ii), or (iv).

4. General form of the fractional tumor-Macrophages interaction model

The general form of the fractional population model involving CF derivative can be written as

$$ {}^{Cf}D_a^{\xi}\varrho_{\varphi}(t) = b_{\varphi}h_{\varphi}(\overline{\varrho}), \tag{4.1}$$

where $\varrho_{\varphi} = (w, x, y, z)^T = (\varrho_{\varphi}^{(0)},\ \varrho_{\varphi}^{(1)},\ \varrho_{\varphi}^{(2)},\ \varrho_{\varphi}^{(3)})^T \in R^4$ represents the vector's state variable of System (5), and the right-hand side of the last equation represents the nonlinear vector function of System (5).

The initial conditions are,

$$\varrho_{\varphi}^{(\rho-1)}(0) = c_{\varphi}, \quad \varphi, \rho = 1, 2, 3, 4. \tag{4.2}$$

at which

$$\overline{\varrho} = \{\varrho_1(t), \varrho_2(t), \varrho_3(t), \varrho_4(t)\}, \quad 0 < \xi < 1.$$

Currently, the fractional integration of order ξ, and take $a = 0$ reduces System (3.3) to the system of fractional integral equations,

$$\varrho_{\varphi}(t) = c_{\varphi} + \frac{1-\xi}{B(\xi)}b_{\varphi}h_{\varphi}(\overline{\varrho}) - \frac{\xi}{B(\xi)}\int_0^t b_{\varphi}h_{\varphi}(\overline{\varrho})\,ds \tag{4.3}$$

Assume that $x_{\varphi}(t)$ is bounded $\forall\ t \in \rho = [0, T]; T \in R^+$, b_{φ} are finite constants; and $h_{\varphi}(\overline{\varrho})$ achieve the Lipschitz condition with Lipschitz constants L_{φ} such as,

$$\left|h_{\varphi}(\overline{\varrho}) - H_{h\varphi}(\overline{\vartheta})\right| \leq L_{\varphi}\left|\overline{\varrho} - \overline{\vartheta}\right| \tag{4.4}$$

and has the Adomian polynomials representation,

$$h_{\varphi}(\overline{\varrho}) = \sum_{\eta=0}^{\infty} A_{\varphi\eta}(\varrho_{\varphi 0}, \varrho_{\varphi 1}, \ldots, \varrho_{\varphi 4}) \tag{4.5}$$

where,

$$A_{\varphi\eta} = \frac{1}{\eta!}\left[\frac{d^{\eta}}{d\lambda^{\eta}}h_{\varphi}\left(\sum_{\rho=0}^{\infty}\lambda^{\rho}\varrho_{\rho}\right)\right]_{\lambda=0} \tag{4.6}$$

Substituting Eq (4.5) into Eq (4.3), we get the following:

$$\varrho_{\varphi}(t) = c_{\varphi} + \frac{1-\xi}{B(\xi)}b_{\varphi}\sum_{\eta=0}^{\infty}A_{\varphi\eta} - \frac{\xi}{B(\xi)}\int_0^t b_{\varphi}\sum_{\eta=0}^{\infty}A_{\varphi\eta}\,ds. \tag{4.7}$$

If we let $\varrho_{\varphi}(t) = \sum_{\eta=0}^{\infty} \varrho_{\varphi\eta}(t)$ in (4.7) , we get

$$\varrho_{\varphi 0}(t) = c_{\varphi}, \tag{4.8}$$

$$\varrho_{\varphi\eta}(t) = \frac{1-\xi}{B(\xi)} b_{\varphi} A_{\varphi(\eta-1)} - \frac{\xi}{B(\xi)} \int_0^t b_{\varphi} A_{\varphi(\eta-1)} ds, \quad \eta \geq 1. \tag{4.9}$$

Lastly, the solution is,

$$\varrho_{\varphi}(t) = \sum_{\eta=0}^{\infty} \varrho_{\varphi\eta}(t). \tag{4.10}$$

5. Convergence analysis for the ADM method

5.1. The uniqueness of the solution

Define the mapping $R : E \to E$, and E is the Banach space $(C^{(n)}(\rho), \|\cdot\|)$, where $C^{(n)}(\rho)$ is the class of all continuous column vectors $\varrho = (\overline{\varrho})'$ with norm $\|\varrho\| = \sum_{\eta=1}^{n} \max_{t\in\rho} \left|\varrho_{\eta}(t)\right|$ and $(.)'$ denote the transpose of the matrix.

Theorem 1. *The systems (4.1) and (4.2)* have *a unique solution at which* $0 < \beta < 1$, $\beta = \frac{LM\left[1+\xi T\right]}{B(\xi)}$ *where* $L = \sum_{m=1}^{n} L_m$, $M = \max\{b_1, b_2, \ldots, b_n\}$.

Proof. Equation (4.3) can be phrased as:

$$\varrho(t) = C + \frac{1-\xi}{B(\xi)} \mathfrak{B} H(\overline{\varrho}) - \frac{\xi}{B(\xi)} \int_0^t \mathfrak{B} H(\overline{\varrho})\, ds$$

where,

$$\begin{aligned} C &= (c_1, c_2, \ldots, c_n)' \\ X(t) &= (x_1, x_2, \ldots, x_n)', \\ \mathfrak{B} &= diag\{b_1, b_2, \ldots, b_n\}, \\ H(\overline{\varrho}(t)) &= (h_1(\overline{\varrho}), h_2(\overline{\varrho}), \ldots, h_n(\overline{\varrho}))'. \end{aligned}$$

The mapping $R : E \to E$ is defined as

$$R\varrho(t) = C + \frac{1-\xi}{B(\xi)} \mathfrak{B} H(\overline{\varrho}) - \frac{\xi}{B(\xi)} \int_0^t \mathfrak{B} H(\overline{\varrho})\, ds.$$

Let $\varrho, \vartheta \in E$:

$$\begin{aligned} \|R\varrho(t) - R\vartheta(t)\| &= \left\| \frac{1-\xi}{B(\xi)} \mathfrak{B}\left(H(\overline{\varrho}) - H(\overline{\vartheta})\right) + \frac{\xi}{B(\xi)} \int_0^t \mathfrak{B}\left(H(\overline{\varrho}) - H(\overline{\vartheta})\right) ds \right\| \\ &\leq \left\| \frac{1-\xi}{B(\xi)} \mathfrak{B}\left(H(\overline{\varrho}) - H(\overline{\vartheta})\right) \right\| + \left\| \frac{\xi}{B(\xi)} \int_0^t \mathfrak{B}\left(H(\overline{\varrho}) - H(\overline{\vartheta})\right) ds \right\| \\ &\leq \frac{1}{B(\xi)} \|\mathfrak{B}\| \left\| H(\overline{\varrho}) - H(\overline{\vartheta}) \right\| + \frac{\xi}{B(\xi)} \int_0^t \|\mathfrak{B}\| \left\| H(\overline{\varrho}) - H(\overline{\vartheta}) \right\| ds \end{aligned}$$

$$
\begin{aligned}
&\leq \frac{M}{B(\xi)}\left(\sum_{m=1}^{n}\max_{t\in\rho}\left|h_m(\overline{\varrho})-h_m(\overline{\vartheta})\right|\right)\\
&\quad+\frac{\xi M}{B(\xi)}\int_0^t\left(\sum_{m=1}^{n}\max_{t\in\rho}\left|h_m(\overline{\varrho})-h_m(\overline{\vartheta})\right|\right)ds\\
&\leq \frac{M}{B(\xi)}\left(\sum_{m=1}^{n}\max_{t\in\rho}\left|h_m(\overline{\varrho})-h_m(\overline{\vartheta})\right|\right)\left[1+\xi\int_0^t ds\right]\\
&\leq \frac{M}{B(\xi)}\left[1+\xi T\right]\sum_{m=1}^{n}L_m\left\|\varrho-\vartheta\right\|\\
&\leq \frac{M\left[1+\xi T\right]}{B(\xi)}\sum_{m=1}^{n}L_m\left\|\varrho-\vartheta\right\|\\
&\leq \frac{M\left[1+\xi T\right]}{B(\xi)}\sum_{m=1}^{n}L_m\left\|\varrho-\vartheta\right\|\\
&\leq \frac{LM\left[1+\xi T\right]}{B(\xi)}\left\|\varrho-\vartheta\right\|\\
&\leq \beta\left\|\varrho-\vartheta\right\|
\end{aligned}
$$

Under Condition $0<\beta<1$, the proof has been proven, as there is a unique solution to Systems (4.1) and (4.2) since the mapping R is a contraction.

5.2. Proof of convergence

Theorem 2. *Using the ADM, the series solution (4.10) of Systems (4.1) and (4.2) converges if* $\left|\varrho_{\varphi 1}\right|<\infty$ *and* $0<\beta<1$ *and* $\beta=\frac{LM\left[1+\xi T\right]}{B(\xi)}$, *where* $L=\sum\limits_{\eta=1}^{n}L_\eta$, $M=\max\{b_1,b_2,\ldots,b_n\}$.

Proof. Define a sequence $\left\{\Theta_{\varphi r}\right\}$ such that, $\Theta_{\varphi r}=\sum\limits_{\eta=0}^{r}\varrho_{\varphi\eta}(t)$ is the series solution's partial sum sequence, $\sum\limits_{\eta=0}^{\infty}\varrho_{\varphi\eta}(t)$. We obtain

$$
h(\Theta_{\varphi r})=\sum_{\eta=0}^{r}A_{\varphi\eta}(\varrho_{\varphi 0},\varrho_{\varphi 1},\ldots,\varrho_{\varphi r})
$$

Let $\Theta_{\varphi r}$ and $\Theta_{\varphi q}$ become two arbitrary partial sums with $r>q$. We are about to show that $\left\{\Theta_{\varphi r}\right\}$ is a Cauchy sequence in this Banach space.

$$
\begin{aligned}
\left\|\Theta_{\varphi r}-\Theta_{\varphi q}\right\| &= \sum_{\eta=1}^{n}\max_{t\in\rho}\left|\Theta_{\eta r}-\Theta_{\eta q}\right|\\
&= \sum_{\eta=1}^{n}\max_{t\in\rho}\left|\sum_{\rho=q+1}^{r}\varrho_{\eta\rho}(t)\right|\\
&\leq \sum_{\eta=1}^{n}\max_{t\in\rho}\left|\sum_{\rho=q+1}^{r}\frac{1-\xi}{B(\xi)}b_\varphi A_{\varphi(\eta-1)}+\frac{\xi}{B(\xi)}\int_0^t b_\varphi A_{\varphi(\eta-1)}ds\right|
\end{aligned}
$$

$$
\begin{aligned}
&\leq \sum_{\eta=1}^{n} \max_{t\in\rho} \left| \frac{1-\xi}{B(\xi)} b_\varphi \sum_{\rho=q+1}^{r} A_{\eta(\rho-1)} + \frac{\xi}{B(\xi)} \int_0^t b_\varphi \sum_{\rho=q+1}^{r} A_{\eta(\rho-1)} ds \right| \\
&\leq \sum_{\eta=1}^{n} \max_{t\in\rho} \left| \frac{1-\xi}{B(\xi)} b_\varphi \sum_{\rho=q}^{r-1} A_{\eta\rho} + \frac{\xi}{B(\xi)} \int_0^t b_\varphi \sum_{\rho=q}^{r-1} A_{\eta\rho} ds \right| \\
&\leq \sum_{\eta=1}^{n} \max_{t\in\rho} \left| \frac{1-\xi}{B(\xi)} b_\varphi [h(\Theta_{\eta(r-1)}) - h(\Theta_{\eta(q-1)})] \right. \\
&\quad \left. + \frac{\xi}{B(\xi)} \int_0^t b_\varphi [h(\Theta_{\eta(r-1)}) - h(\Theta_{\eta(q-1)})] ds \right| \\
&\leq \sum_{\eta=1}^{n} \max_{t\in\rho} \left[\left| \frac{1-\xi}{B(\xi)} b_\varphi [h(\Theta_{\eta(r-1)}) - h(\Theta_{\eta(q-1)})] \right| \right. \\
&\quad \left. + \left| \frac{\xi}{B(\xi)} \int_0^t b_\varphi [h(\Theta_{\eta(r-1)}) - h(\Theta_{\eta(q-1)})] ds \right| \right]
\end{aligned}
$$

$$
\begin{aligned}
&\leq \sum_{\eta=1}^{n} \max_{t\in\rho} \left[\frac{1-\xi}{B(\xi)} \left| b_\varphi \right| \left| h(\Theta_{\eta(r-1)}) - h(\Theta_{\eta(q-1)}) \right| \right. \\
&\quad \left. + \frac{\xi}{B(\xi)} \int_0^t \left| b_\varphi \right| \left| h(\Theta_{\eta(r-1)}) - h(\Theta_{\eta(q-1)}) \right|] d\Theta \right] \\
&\leq \sum_{\eta=1}^{n} \max_{t\in\rho} \left[\frac{1-\xi}{B(\xi)} \left| b_\varphi \right| \left(L_\eta \sum_{\rho=1}^{n} \left| \Theta_{\rho(r-1)} - \Theta_{\rho(q-1)} \right| \right) \right. \\
&\quad \left. + \frac{\xi}{B(\xi)} \int_0^t \left| b_\varphi \right| \left(L_\eta \sum_{\rho=1}^{n} \left| \Theta_{\rho(r-1)} - \Theta_{\rho(q-1)} \right| \right) d\Theta \right] \\
&\leq \sum_{\eta=1}^{n} \max_{t\in\rho} \left(L_\eta \sum_{\rho=1}^{n} \left| \Theta_{\rho(r-1)} - \Theta_{\rho(q-1)} \right| \right) \left[\frac{1}{B(\xi)} M + \frac{\xi M}{B(\xi)} \int_0^t ds \right] \\
&\leq \sum_{\eta=1}^{n} \max_{t\in\rho} \left(L_\eta \sum_{\rho=1}^{n} \left| \Theta_{\rho(r-1)} - \Theta_{\rho(q-1)} \right| \right) \left[\frac{1}{B(\xi)} M + \frac{\xi M}{B(\xi)} \int_0^t ds \right] \\
&\leq \frac{LM[1+\xi T]}{B(\xi)} \left\| \Theta_{\varphi(r-1)} - \Theta_{\varphi(q-1)} \right\| \\
&\leq \beta \left\| \Theta_{\varphi(r-1)} - \Theta_{\varphi(q-1)} \right\|
\end{aligned}
$$

Let $r = q + 1$, then

$$
\left\| \Theta_{\varphi(q+1)} - \Theta_{\varphi q} \right\| \leq \beta \left\| \Theta_{\varphi q} - \Theta_{\varphi(q-1)} \right\| \leq \beta^2 \left\| \Theta_{\varphi(q-1)} - \Theta_{\varphi(q-2)} \right\| \leq \cdots \leq \beta^q \left\| \Theta_{\varphi 1} - \Theta_{\varphi 0} \right\|
$$

Using the triangle inequality we have

$$
\begin{aligned}
\left\| \Theta_{\varphi r} - \Theta_{\varphi q} \right\| &\leq \left\| \Theta_{\varphi(q+1)} - \Theta_{\varphi q} \right\| + \left\| \Theta_{\varphi(q+2)} - \Theta_{\varphi(q+1)} \right\| + \cdots + \left\| \Theta_{\varphi r} - \Theta_{\varphi(r-1)} \right\| \\
&\leq \left[\beta^q + \beta^{q+1} + \cdots + \beta^{r-1} \right] \left\| \Theta_{\varphi 1} - \Theta_{\varphi 0} \right\|
\end{aligned}
$$

$$\begin{aligned} &\leq \beta^q \left[1+\beta+\cdots+\beta^{r-q-1}\right] \left\|\Theta_{\varphi 1}-\Theta_{\varphi 0}\right\| \\ &\leq \beta^q \left[\frac{1-\beta^{r-q}}{1-\beta}\right] \left\|\varrho_{\varphi 1}(t)\right\| \end{aligned}$$

Given that, $0<\beta<1$ and $r>q$, then $(1-\beta^{r-q}) \leq 1$. Therefore

$$\begin{aligned} \left\|\Theta_{\varphi r}-\Theta_{\varphi q}\right\| &\leq \frac{\beta^q}{1-\beta}\left\|\varrho_{\varphi 1}(t)\right\| \\ &\leq \frac{\beta^q}{1-\beta}\max_{t\in\rho}\left|\varrho_{\varphi 1}(t)\right| \quad , \end{aligned}$$

but, $\left|\varrho_{\varphi 1}(t)\right|<\infty$ and as $q\to\infty$, then $\left\|\Theta_{\varphi r}-\Theta_{\varphi q}\right\|\to 0$ and hence $\left\{\Theta_{\varphi r}\right\}$ is a Cauchy sequence in this Banach space, so the series $\sum_{\eta=0}^{\infty}\varrho_{\varphi\eta}(t)$ converges and the proof is complete.

5.3. Error analysis

The following theorem allows us to estimate the maximum absolute truncation error of the Adomian series' solution.

Theorem 3. *The maximum absolute truncation error of the series solution (4.10) to Systems (4.1) and (4.2) is calculated to be:*

$$\max_{t\in\rho}\left|\varrho_{\varphi}(t)-\sum_{\eta=0}^{q}\varrho_{\varphi\eta}(t)\right| \leq \frac{\beta^q}{1-\beta}\max_{t\in\rho}\left|\varrho_{\varphi 1}(t)\right|.$$

Proof. From Theorem 2, we get

$$\left\|\Theta_{\varphi r}-\Theta_{\varphi q}\right\| \leq \frac{\beta^q}{1-\beta}\max_{t\in\rho}\left|\varrho_{\varphi 1}(t)\right|.$$

On the other hand, $\Theta_{\varphi r}=\sum_{\eta=0}^{r}\varrho_{\varphi\eta}(t)$ as $r\to\infty$, then $\Theta_{\varphi r}\to\varrho_{\varphi}(t)$ so,

$$\left\|\varrho_{\varphi}(t)-\Theta_{\varphi q}\right\| \leq \frac{\beta^q}{1-\beta}\max_{t\in\rho}\left|\varrho_{\varphi 1}(t)\right|.$$

Therefore, the maximum absolute truncation error in the interval ρ is

$$\max_{t\in\rho}\left|\varrho_{\varphi}(t)-\sum_{\eta=0}^{q}\varrho_{\varphi\eta}(t)\right| \leq \frac{\beta^q}{1-\beta}\max_{t\in\rho}\left|\varrho_{\varphi 1}(t)\right|$$

and this completes the proof.

6. The Picard method

In the context of applying the PM to Eq (4.7), the solution is constructed iteratively through a sequence of functions defined as follows:

$$\begin{aligned} \varrho_{\varphi 0}(t) &= c_{\varphi}, \\ \varrho_{\varphi\eta}(t) &= \varrho_{\varphi 0}(t) + \frac{1-\xi}{B(\xi)} d_{\varphi} h_{\varphi(\eta-1)}\left(\overline{\varrho}_{\eta-1}\right) - \frac{\xi}{B(\xi)} \int_0^t d_{\varphi} h_{\varphi}\left(\overline{\varrho}_{\eta-1}\right) ds, \quad \eta \geq 1. \end{aligned} \tag{6.1}$$

Equation (6.1) can be expressed as

$$\begin{aligned} \varrho_0(t) &= C, \\ \varrho_{\eta}(t) &= \frac{1-\xi}{B(\xi)} \mathfrak{D} H\left(\overline{\varrho}_{\eta-1}\right) - \frac{\xi}{B(\xi)} \int_0^t \mathfrak{D} H\left(\overline{\varrho}_{\eta-1}\right) ds, \end{aligned}$$

where

$$\begin{aligned} C &= (c_1, c_2, \ldots, c_n)', \\ \varrho(t) &= (\varrho_1, \varrho_2, \ldots, \varrho_n)', \\ \mathfrak{D} &= diag\{d_1, d_2, \ldots, d_n\}, \\ H(\overline{\varrho}(t)) &= (h_1(\overline{\varrho}), h_2(\overline{\varrho}), \ldots, h_n(\overline{\varrho}))'. \end{aligned}$$

All the vector functions $\varrho_{\eta}(t)$ are continuous, and each ϱ_{η} can be expressed as a series of successive differences as follows:

$$\varrho_{\eta} = \varrho_0 + \sum_{\rho=1}^{n} (\varrho_{\rho} - \varrho_{\rho-1}).$$

This indicates that the convergence of the sequence ϱ_{η} is directly related to the convergence of the infinite series $\sum(\varrho_{\rho} - \varrho_{\rho-1})$. Consequently, the solution can be expressed as:

$$\varrho(t) = \lim_{\rho\to\infty} \varrho_{\rho}(t),$$

In other words, if the infinite series $\sum(\varrho_{\rho} - \varrho_{\rho-1})$ converges, the sequence $\varrho_{\rho}(t)$ converges to $\varrho(t)$. To demonstrate the convergence of set $\{\varrho_{\rho}(t)\}$, we will examine the following related series:

$$\sum_{\rho=1}^{\infty} [\varrho_{\rho}(t) - \varrho_{\rho-1}(t)].$$

From (4.2) , for $\rho = 1$, we have:

$$\varrho_1(t) - \varrho_0(t) = \frac{1-\xi}{B(\xi)} \mathfrak{D} H(\overline{\varrho}_0) - \frac{\xi}{B(\xi)} \int_0^t \mathfrak{D} H(\overline{\varrho}_0)\, ds.$$

We have:

$$|\varrho_1(t) - \varrho_0(t)| \leq \left|\frac{1-\xi}{B(\xi)} \mathfrak{D} H(\overline{\varrho}_0)\right| + \left|\frac{\xi}{B(\xi)} \int_0^t \mathfrak{D} H(\overline{\varrho}_0)\, ds\right|$$

$$\begin{aligned} &\leq \frac{1}{B(\xi)}|\mathfrak{D}|\left|H(\overline{\varrho}_0)\right| + \frac{\xi}{B(\xi)}\int_0^t |\mathfrak{D}|\left|H(\overline{\varrho}_0)\right| ds \\ &\leq MM_2\left[\frac{1}{B(\xi)} + \frac{\xi}{B(\xi)}\int_0^t ds\right] \end{aligned}$$

where $|H(\overline{\varrho})| < M_2$, $|\mathfrak{D}| < M$, and hence, we get

$$\begin{aligned} |\varrho_1(t) - \varrho_0(t)| &\leq \frac{MM_2}{B(\xi)}[1 + \xi T] \\ &\leq \frac{M_2}{L}\beta, \end{aligned}$$

Now, we will derive an estimate for $\varrho_\rho(t) - \varrho_{\rho-1}(t)$ for $\rho \geq 2$.

$$\begin{aligned} \varrho_\rho(t) - \varrho_{\rho-1}(t) &= \frac{1-\xi}{B(\xi)}\mathfrak{D}H\left(\overline{\varrho}_{\rho-1}\right) - \frac{\xi}{B(\xi)}\int_0^t \mathfrak{D}H\left(\overline{\varrho}_{\rho-1}\right) ds \\ &\quad -\left[\frac{1-\xi}{B(\xi)}\mathfrak{D}H\left(\overline{\varrho}_{\rho-2}\right) - \frac{\xi}{B(\xi)}\int_0^t \mathfrak{D}H\left(\overline{\varrho}_{\rho-2}\right) ds\right] \\ &= \left[\frac{1-\xi}{B(\xi)}\mathfrak{D}\left[H\left(\overline{\varrho}_{\rho-1}\right) - H\left(\overline{\varrho}_{\rho-2}\right)\right]\right] - \left[\frac{\xi}{B(\xi)}\int_0^t \mathfrak{D}\left[H\left(\overline{\varrho}_{\rho-1}\right) - H\left(\overline{\varrho}_{\rho-2}\right)\right] ds\right] \\ \left|\varrho_\rho(t) - \varrho_{\rho-1}(t)\right| &\leq \left|\frac{1-\xi}{B(\xi)}\mathfrak{D}\left[H\left(\overline{\varrho}_{\rho-1}\right) - H\left(\overline{\varrho}_{j-2}\right)\right]\right| + \left|\frac{\xi}{B(\xi)}\int_0^t \mathfrak{D}\left[H\left(\overline{\varrho}_{\rho-1}\right) - H\left(\overline{\varrho}_{j-2}\right)\right] ds\right|, \end{aligned}$$

To derive the estimate for $|\varrho_\rho(t) - \varrho_{\rho-1}(t)|$, we start with the inequality:

$$\begin{aligned} \left|\varrho_j(t) - \varrho_{j-1}(t)\right| &\leq \frac{1}{B(\xi)}|\mathfrak{D}|\left|H\left(\overline{\varrho}_{\rho-1}\right) - H\left(\overline{\varrho}_{\rho-2}\right)\right| \\ &\quad + \frac{\xi}{B(\xi)}\int_0^t |\mathfrak{D}|\left|H\left(\overline{\varrho}_{\rho-1}\right) - H\left(\overline{\varrho}_{\rho-2}\right)\right| ds \\ &\leq \frac{M}{B(\xi)}\left[1 + \xi\int_0^t ds\right]\left|H\left(\overline{\varrho}_{\rho-1}\right) - H\left(\overline{\varrho}_{\rho-2}\right)\right| \\ &\leq \frac{ML}{B(\xi)}[1 + \xi T]\left|\overline{\varrho}_{\rho-1} - \overline{\varrho}_{\rho-2}\right| \\ &\leq \beta\left|\varrho_{\rho-1} - \varrho_{\rho-2}\right|. \end{aligned} \tag{6.2}$$

Putting $\rho = 2$ into this inequality, we can use the previous result to establish a recursive relationship:

$$|\varrho_2(t) - \varrho_1(t)| \leq \beta|\varrho_1(t) - \varrho_0(t)|.$$

From (4.4), we obtain

$$\begin{aligned} |\varrho_2(t) - \varrho_1(t)| &\leq \beta|\varrho_1(t) - \varrho_0(t)| \\ &\leq \beta^2\frac{M_2}{L}. \end{aligned}$$

Applying the same method for $n = 3, 4, \ldots$ and so on, we derive

$$|\varrho_3(t) - \varrho_2(t)| \leq \beta|\varrho_2(t) - \varrho_1(t)|$$

$$\leq \beta^3 \frac{M_2}{L}.$$

By applying this method repeatedly, we arrive at the following general estimate for the series terms:

$$|\varrho_\rho - \varrho_{\rho-1}| \leq \beta^j \frac{M_2}{L} \tag{6.3}$$

Given that $0 < \beta < 1$, it follows that the uniform convergence of

$$\sum_{\rho=1}^{\infty} \left[\varrho_\rho(t) - \varrho_{\rho-1}(t)\right]$$

is established, indicating that the sequence $\{\varrho_\rho(t)\}$ converges uniformly. As $H(\overline{\varrho})$ is continuous in $\overline{\varrho}$, it follows that

$$\begin{aligned} \varrho(t) &= \lim_{\eta\to\infty} \frac{1-\xi}{B(\xi)} \mathfrak{D} H(\overline{\varrho}_k) - \frac{\xi}{B(\xi)} \int_0^t \mathfrak{D} H(\overline{\varrho}_k)\, ds \\ &= \lim_{\eta\to\infty} \frac{1-\xi}{B(\xi)} \mathfrak{D} H(\overline{\varrho}) - \frac{\xi}{B(\xi)} \int_0^t \mathfrak{D} H(\overline{\varrho})\, ds. \end{aligned}$$

Hence, it is verified that a solution exists.

To demonstrate uniqueness, assume that $\varrho(t)$ be a continuous solution of the system. Consequently, we have:

$$X(t) = C + \frac{1-\xi}{B(\xi)} \mathfrak{D} H(\overline{x}) - \frac{\xi}{B(\xi)} \int_0^t \mathfrak{D} H(\overline{x})\, ds, \quad t \in [0,1],$$

and we obtain the following estimates:

$$\begin{aligned} |\chi(t) - \varrho_j(t)| &\leq \left|\frac{1-\xi}{B(\xi)} \mathfrak{D}\left[H(\overline{\varkappa}) - H\left(\overline{\varrho}_{\rho-1}\right)\right]\right| - \left|\frac{\xi}{B(\xi)} \int_0^t \mathfrak{D}\left[H(\overline{\varkappa}) - H\left(\overline{\varrho}_{\rho-1}\right)\right] ds\right| \\ &\leq \frac{1}{B(\xi)} |\mathfrak{D}| \left|H(\overline{\varkappa}) - H\left(\overline{y}_{\rho-1}\right)\right| - \frac{\xi}{B(\xi)} \int_0^t |\mathfrak{D}| \left|H(\overline{\varkappa}) - H\left(\overline{\varrho}_{\rho-1}\right)\right| ds \\ &\leq \frac{1-\xi}{B(\xi)} ML \left|\overline{\varkappa} - \overline{\varrho}_{\rho-1}\right| - \frac{\xi}{B(\xi)} ML \left|\overline{\varkappa} - \overline{\varrho}_{\rho-1}\right| \int_0^t ds \\ &\leq \frac{[1-\xi T]}{B(\xi)} ML \left|\overline{\varkappa} - \overline{\varrho}_{\rho-1}\right| \\ &\leq \beta \left|\overline{\varkappa} - \overline{\varrho}_{\rho-1}\right| \end{aligned}$$

But

$$\begin{aligned} |\chi(t) - \varrho_0(t)| &\leq \frac{1-\xi}{B(\xi)} |\mathfrak{D}| \left|H(\overline{\varkappa})\right| + \frac{\xi}{B(\xi)} \int_0^t |\mathfrak{D}| \left|H(\overline{\varkappa})\right| ds \\ &\leq \frac{1}{B(\xi)} |\mathfrak{D}| \left|H(\overline{\varkappa})\right| + \frac{\xi}{B(\xi)} \int_0^t |\mathfrak{D}| \left|H(\overline{\varkappa})\right| ds \\ &\leq \frac{1}{B(\xi)} M M_2 + \frac{\xi}{B(\xi)} M M_2 T \end{aligned}$$

$$\begin{aligned} &\leq \frac{MM_2(1+\xi T)}{B(\xi)} \\ &\leq \frac{M_2}{L}\beta. \end{aligned}$$

Using (6.3), we derive

$$\begin{aligned} |\chi(t)-\varrho_j(t)| &\leq \beta|\chi(t)-\varrho_{j-1}(t)| \\ &\leq \beta^j\frac{M_2}{L}. \end{aligned}$$

Therefore

$$\lim_{j\to\infty}\varrho_j(t)=\chi(t)=\varrho(t).$$

This concludes the proof.

7. The Adomian decomposition method

Using the ADM, we can find the solution to System (3.3) in a recurrence relation as follows

$$\begin{aligned} T_0 &= T(0),\ T_{j+1}=\alpha_1\,{}^{Cf}I^{\xi}\left[T_j-\beta_1A_j\right]-\gamma_1\,{}^{Cf}I^{\xi}\,B_j+\delta_1\,{}^{Cf}I^{\xi}\,C_j-\mu_1\,{}^{Cf}I^{\xi}\,D_j,\\ M_{1_0} &= M_1(0),\ M_{1_{j+1}}=\alpha_2\,{}^{Cf}I^{\xi}B_j-\beta_2\,{}^{Cf}I^{\xi}M_{1_j}-\gamma_2\,{}^{Cf}I^{\xi}M_{1_j}+\delta_2\,{}^{Cf}I^{\xi}M_{2_j}-\mu_2\,{}^{Cf}I^{\xi}E_j,\\ M_{2_0} &= M_2(0),\ M_{2_{j+1}}=\alpha_3\,{}^{Cf}I^{\xi}C_j-\beta_3\,{}^{Cf}I^{\xi}M_{2_j}+\gamma_2\,{}^{Cf}I^{\xi}M_{1_j}-\delta_2\,{}^{Cf}I^{\xi}M_{2_j}-\mu_3\,{}^{Cf}I^{\xi}G_j,\\ F_0 &= F(0),\ F_{j+1}=-\mu_4\,{}^{Cf}I^{\xi}F_j+\mu_5\,{}^{Cf}I^{\xi}T_j. \end{aligned} \tag{7.1}$$

These series are introduced in accordance with the ADM's assumptions:

$$T(t)=\sum_{j=0}^{n}T_j(t),\ M_1(t)=\sum_{j=0}^{n}M_{1j}(t),\ M_2(t)=\sum_{j=0}^{n}M_{2j}(t),\ F(t)=\sum_{j=0}^{n}F_j(t),$$

where a description of the sum of the nonlinear components is obtained as follows:

$$\begin{aligned} {M_1}^2(t) &= \sum_{j=0}^{n}A_j,\ T(t)M_1(t)=\sum_{j=0}^{n}B_j,\ T(t)M_2(t)=\sum_{j=0}^{n}C_j,\\ T(t)F(t) &= \sum_{j=0}^{n}D_j,\ M_1(t)F(t)=\sum_{j=0}^{n}E_j,\ M_2(t)F(t)=\sum_{j=0}^{n}G_j. \end{aligned}$$

where $n=0,1,2,\ldots,n$.

The Adomian polynomials A_j, B_j, C_j, D_j, E_j , and G_j are obtained from (4.6) as follows:

$$\begin{array}{ccc} A_0=M_{1_0}^2, & B_0=M_{1_0}T_0 & C_0=M_{2_0}T_0\\ A_1=2M_{1_0}M_{1_1}, & B_1=M_{1_0}T_1+M_{1_1}T_0 & C_1=M_{2_0}T_1+M_{2_1}T_0\\ A_2=M_{1_1}^2+2M_{1_0}M_{1_2}, & B_2=M_{1_0}T_2+M_{1_1}T_1+M_{1_2}T_0 & C_2=M_{2_0}T_2+M_{2_1}T_1+M_{2_2}T_0\\ \ldots & \ldots & \ldots \end{array}$$

$$\begin{array}{ccc} D_0 = F_0T_0 & E_0 = M_{1_0}F_0 & G_0 = M_{2_0}F_0 \\ D_1 = F_0T_1 + F_1T_0 & E_1 = M_{1_0}F_1 + M_{1_1}F_0 & G_1 = M_{2_0}F_1 + M_{2_1}F_0 \\ D_2 = F_0T_2 + F_1T_1 + F_2T_0 & E_2 = M_{1_0}F_2 + M_{1_1}F_1 + M_{1_2}F_0 & G_2 = M_{2_0}F_2 + M_{2_1}F_1 + M_{2_2}F_0 \\ \cdots & \cdots & \cdots \end{array}$$

Substituting equalities into System (7.1) yields the following results:

$$\begin{aligned} \sum_{j=0}^{n} T_j(t) &= T(0) + \alpha_1\, {}^{Cf}I^{\xi}\left[\sum_{j=0}^{n} T_j - \beta_1 \sum_{j=0}^{n} A_j\right] - \gamma_1\, {}^{Cf}I^{\xi} \sum_{j=0}^{n} B_j + \delta_1\, {}^{Cf}I^{\xi} \sum_{j=0}^{n} C_j - \mu_1\, {}^{Cf}I^{\xi} \sum_{j=0}^{n} D_j, \\ \sum_{j=0}^{n} M_{1_j}(t) &= M_1(0) + \alpha_2\, {}^{Cf}I^{\xi} \sum_{j=0}^{n} B_j - \beta_2\, {}^{Cf}I^{\xi} \sum_{j=0}^{n} M_{1_j} - \gamma_2\, {}^{Cf}I^{\xi} \sum_{j=0}^{n} M_{1_j} + \delta_2\, {}^{Cf}I^{\xi} \sum_{j=0}^{n} M_{2_j} - \mu_2\, {}^{Cf}I^{\xi} \sum_{j=0}^{n} E_j, \\ \sum_{j=0}^{n} M_{2_j}(t) &= M_2(0) + \alpha_3\, {}^{Cf}I^{\xi} \sum_{j=0}^{n} C_j - \beta_3\, {}^{Cf}I^{\xi} \sum_{j=0}^{n} M_{2_j} + \gamma_2\, {}^{Cf}I^{\xi} \sum_{j=0}^{n} M_{1_j} - \delta_2\, {}^{Cf}I^{\xi} \sum_{j=0}^{n} M_{2_j} - \mu_3\, {}^{Cf}I^{\xi} \sum_{j=0}^{n} G_j, \\ \sum_{j=0}^{n} F_j(t) &= F(0) - \mu_4\, {}^{Cf}I^{\xi} \sum_{j=0}^{n} F_j + \mu_5\, {}^{Cf}I^{\xi} \sum_{j=0}^{n} T_j. \end{aligned}$$

At $\xi = 1$, the results can be obtained in the following form for 10 terms:

$$\begin{aligned} T(t) &= 1 - 0.435002t + 0.069614t^2 + 0.00482228t^3 - 0.00457172t^4 + 0.000887607t^5 - \\ &\quad 0.0000174647t^6 - 0.0000309603t^7 + 7.53167 * 10^{-6}t^8 - 5.04832 * 10^{-7}t^9 - 1.62395 * 10^{-7}t^{10}, \\ M_1(t) &= 1 - 0.709999t + 0.249909t^2 - 0.0526546t^3 + 0.00596902t^4 + 0.000118906t^5 - \\ &\quad 0.000183454t^6 + 0.0000318473t^7 - 8.15854 * 10^{-7}t^8 - 7.794 * 10^{-7}t^9 + 1.76437 * 10^{-7}t^{10} \\ M_2(t) &= 1 - 0.191999t + 0.00543163t^2 + 0.00374878t^3 - 0.000888681t^4 + 0.000102849t^5 - \\ &\quad 3.082 * 10^{-6}t^6 - 1.22373 * 10^{-6}t^7 + 2.38171 * 10^{-7}t^8 - 1.08531 * 10^{-8}t^9 - 3.70243 * 10^{-9}t^{10} \\ F(t) &= 1. + 0.05t - 0.0230001t^2 + 0.0027038t^3 + 0.0000867595t^4 - 0.0000923019t^5 + \\ &\quad 0.0000155626t^6 - 3.60658 * 10^{-7}t^7 - 3.84749 * 10^{-7}t^8 + 8.58228 * 10^{-8}t^9 - 5.47743 * 10^{-9}t^{10}. \end{aligned}$$

For $\xi = \frac{1}{2}$, the results are given as follows:

$$\begin{aligned} T(t) &= 0.783271 - 0.172097t + 0.0193621t^2 - 0.00151882t^3 - 0.0002269t^4 - 0.000127007t^5 - \\ &\quad 0.0000458416t^6 - 8.80863 * 10^{-6}t^7 - 1.017 * 10^{-6}t^8 - 5.78326 * 10^{-8}t^9 - 1.20429 * 10^{-9}t^{10}, \\ M_1(t) &= 0.697776 - 0.208576t + 0.0336451t^2 - 0.00282947t^3 + 0.000428758t^4 + 0.0000313639t^5 + \\ &\quad 0.0000184272t^6 + 5.20203 * 10^{-6}6t^7 + 7.34263 * 10^{-7}t^8 + 5.11143 * 10^{-8}t^9 + 1.30842 * 10^{-9}t^{10} \\ M_2(t) &= 0.889519 - 0.101845t + 0.00455165t^2 - 0.0000807398t^3 - 0.0000418569t^4 - 2.3056 * 10^{-6}t^5 - \\ &\quad 5.3811 * 10^{-7}t^6 - 1.03894 * 10^{-7}t^7 - 1.72758 * 10^{-8}t^8 - 1.20298 * 10^{-9}t^9 - 2.74563 * 10^{-11}t^{10} \\ F(t) &= 1.01683 + 0.00610226t - 0.00406187t^2 + 0.000325745t^3 - 0.0000387796t^4 - 6.69621 * 10^{-6}t^5 - \\ &\quad 1.8108 * 10^{-6}t^6 - 2.81895 * 10^{-7}t^7 - 2.69855 * 10^{-8}t^8 - 1.63980 * 10^{-9}t^9 - 4.06193 * 10^{-11}t^{10}. \end{aligned}$$

Figures 1–4 illustrate the solutions obtained from the ADM at different values of ξ (specifically $\xi = 1, 0.9, 0.8, 0.7, 0.6$, and 0.5). These figures visually represent how the solutions change with different

fractional orders. Figures 5–8 gives the solutions of the PM at different values of ξ (specifically $\xi = 1, 0.9, 0.8, 0.7, 0.6,$ and 0.5). Tables 2–5 give a detailed comparison of the absolute error between the solutions obtained using the PM and ADM for a specific case where $\kappa = m = 7$ and $\xi = 1$. This table highlights how closely each method approximates the exact solution at various values of t. Furthermore, Figures 9–12 show the solutions of the two methods at $\xi = 0.5$ and 1.

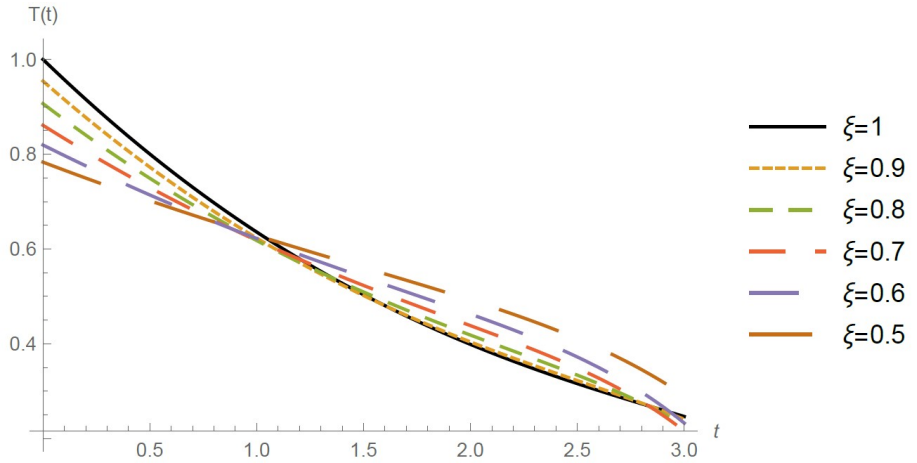

Figure 1. The ADM's solutions of $T(t)$ for several values of ξ from (3.3).

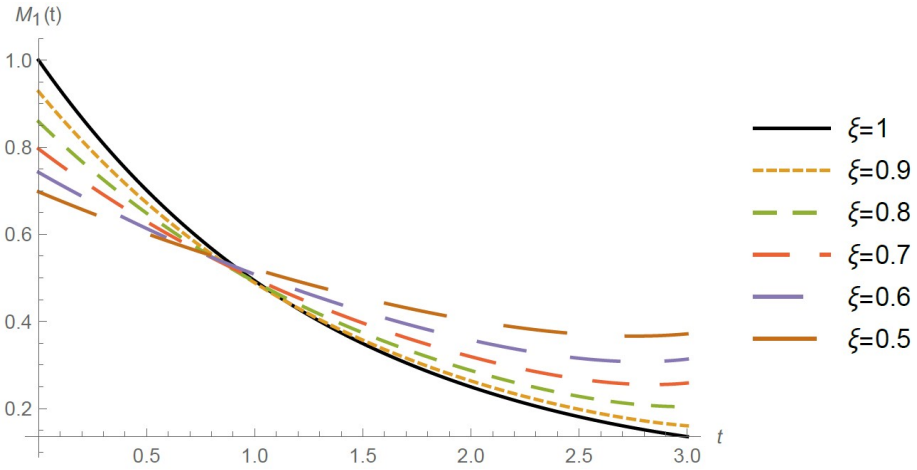

Figure 2. The ADM's solutions of $M_1(t)$ for several values of ξ from (3.3).

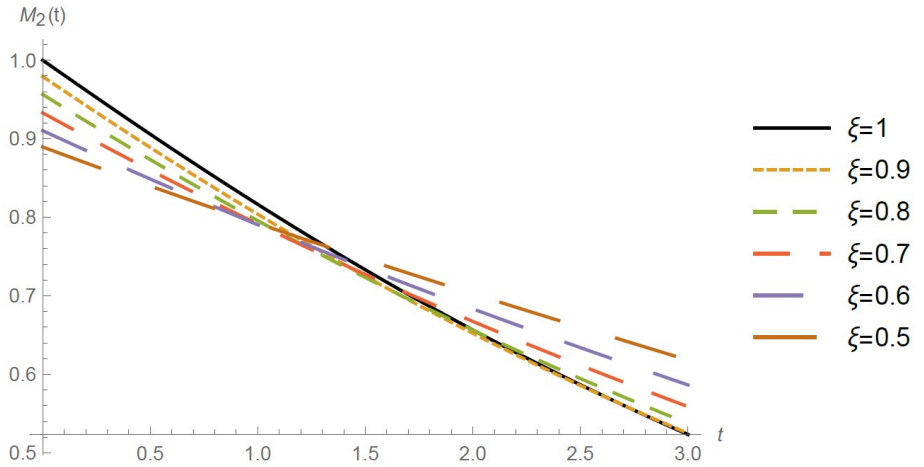

Figure 3. The ADM's solutions of $M_2(t)$ for several values of ξ from (3.3).

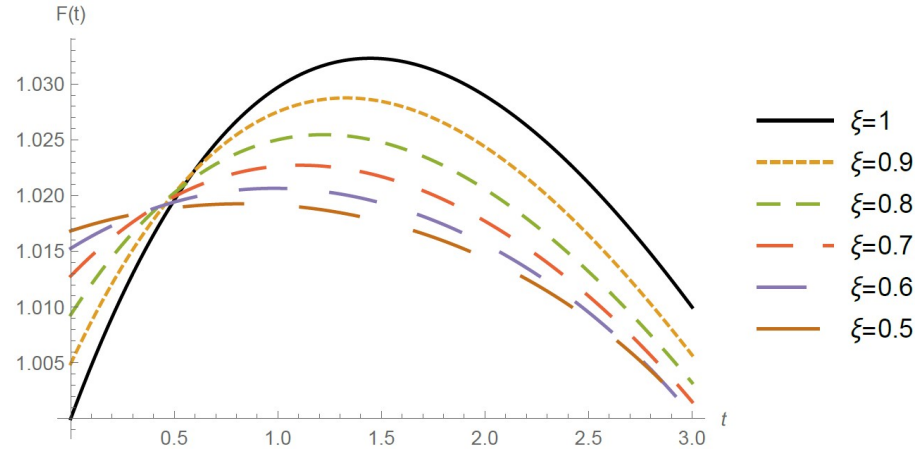

Figure 4. The ADM's solutions of $F(t)$ for several values of ξ from (3.3).

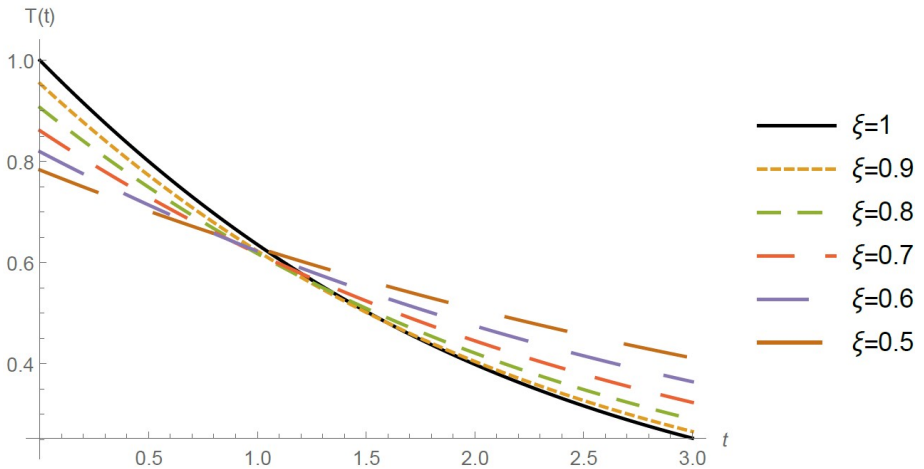

Figure 5. The PM's solutions of $T(t)$ for several values of ξ from (3.3).

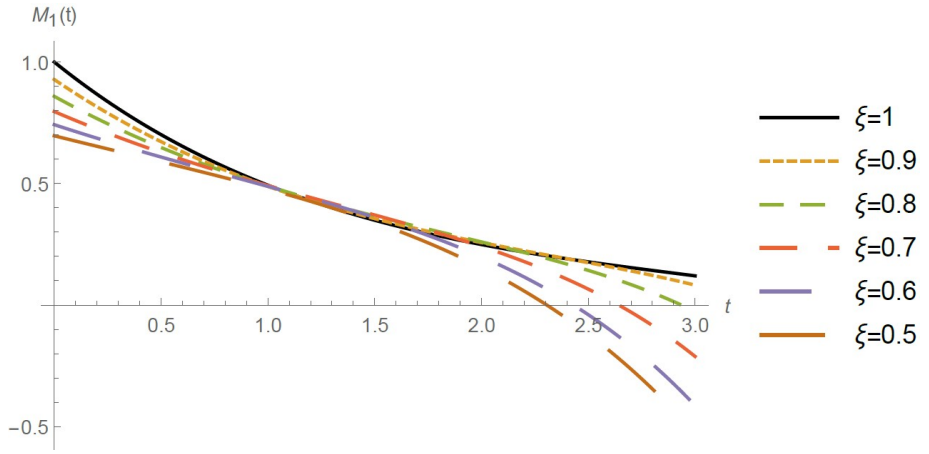

Figure 6. The PM's solutions of $M_1(t)$ for several values of ξ from (3.3).

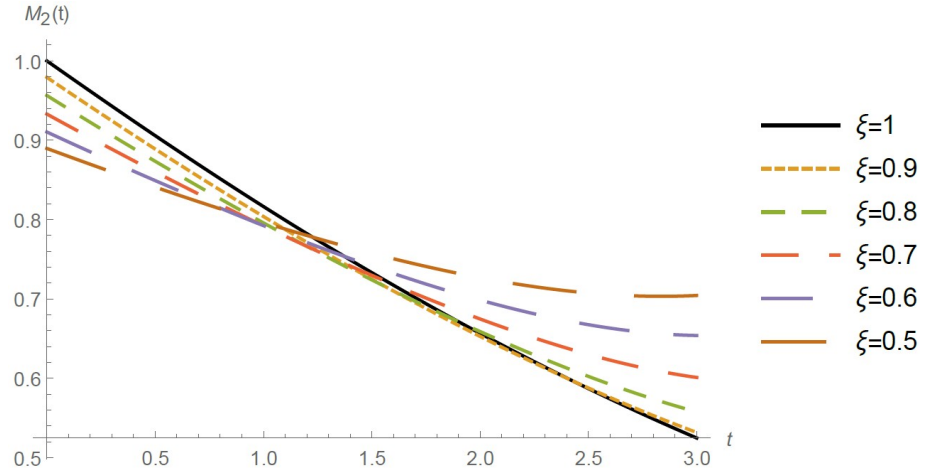

Figure 7. The PM's solutions of $M_2(t)$ for several values of ξ from (3.3).

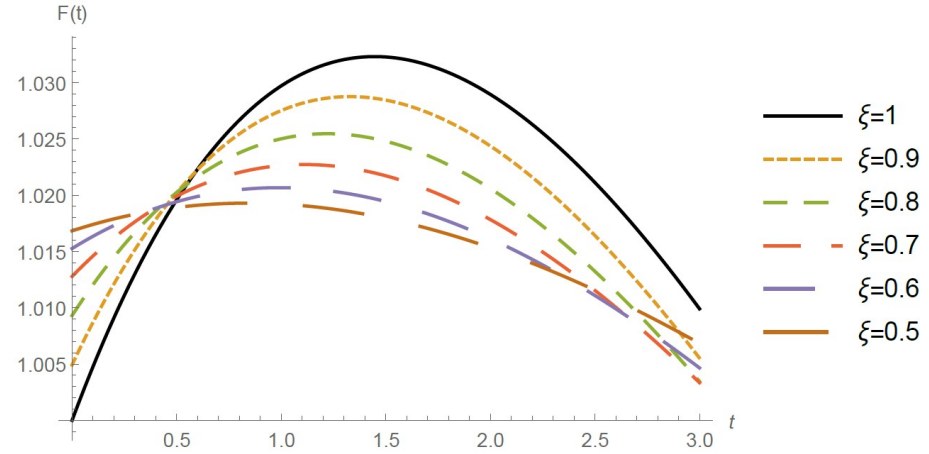

Figure 8. The PM's solutions of $F(t)$ for several values of ξ from (3.3).

Table 2. Absolute difference of $T(t)$ *at* $\xi = 1$ for Problem (3.3).

t	ADM	PM	$AD\vert$
0.1	0.95720032420	0.95720032420	3.70765×10^{-17}
0.2	0.91581572707	0.91581572707	4.47792×10^{-15}
0.3	0.87586000093	0.87586000093	5.86842×10^{-15}
0.4	0.83733804594	0.83733804594	1.78465×10^{-12}
0.5	0.80024686081	0.80024686083	2.51057×10^{-11}
0.6	0.76457648720	0.76457648739	1.92328×10^{-10}
0.7	0.73031090144	0.73031090248	1.03936×10^{-9}
0.8	0.69742884850	0.69742885293	4.42675×10^{-9}
0.9	0.66590461491	0.66590463072	1.58101×10^{-8}
1	0.63570873799	0.63570878724	4.92528×10^{-8}

Table 3. Absolute difference of $M_1(t)$ at $\xi = 1$ for Problem (3.3).

t	ADM	PM	$AD\vert$
0.1	0.93144713398	0.93144713398	2.91800×10^{-12}
0.2	0.86758490292	0.86758490290	2.69289×10^{-11}
0.3	0.80811895250	0.80811895229	2.05042×10^{-10}
0.4	0.75276927948	0.75276927795	1.52501×10^{-9}
0.5	0.70127009616	0.70127008766	8.49772×10^{-9}
0.6	0.65336960801	0.65336957210	3.59157×10^{-8}
0.7	0.60882971832	0.60882959557	1.22751×10^{-7}
0.8	0.56742567237	0.56742531523	3.57134×10^{-7}
0.9	0.52894565303	0.52894473578	9.17252×10^{-7}
1	0.49319033857	0.49318820463	2.13395×10^{-6}

Table 4. Absolute difference of $M_2(t)$ at $\xi = 1$ for Problem (3.3).

t	ADM	PM	$AD\vert$
0.1	0.98085806727	0.98085806510	2.17659×10^{-9}
0.2	0.96184604640	0.96184603828	8.12917×10^{-9}
0.3	0.94298338322	0.94298336616	1.70677×10^{-8}
0.4	0.92428763182	0.92428760359	2.82259×10^{-8}
0.5	0.90577457065	0.90577453006	4.05951×10^{-8}
0.6	0.88745831501	0.88745826274	5.22718×10^{-8}
0.7	0.86935142551	0.86935136638	5.91327×10^{-8}
0.8	0.85146501242	0.85146495995	5.24709×10^{-8}
0.9	0.83380883557	0.83380882042	1.51471×10^{-8}
1	0.81639139968	0.81639148395	8.42698×10^{-8}

Table 5. Absolute difference of $F(t)$ at $\xi = 1$ for Problem (3.3).

t	ADM	PM	$\lvert AD \rvert$
0.1	1.00477271062	1.00477271062	8.67362×10^{-18}
0.2	1.00910173688	1.00910173688	2.58474×10^{-15}
0.3	1.01300348381	1.01300348381	7.56981×10^{-14}
0.4	1.01649436695	1.01649436695	8.50445×10^{-13}
0.5	1.01959072859	1.01959072859	5.65164×10^{-12}
0.6	1.02230876413	1.02230876410	2.69861×10^{-11}
0.7	1.02466445782	1.02466445772	1.02729×10^{-10}
0.8	1.02667352766	1.02667352732	3.3167×10^{-10}
0.9	1.02835137843	1.02835137749	9.44828×10^{-10}
1	1.02971306262	1.02971306018	2.43889×10^{-9}

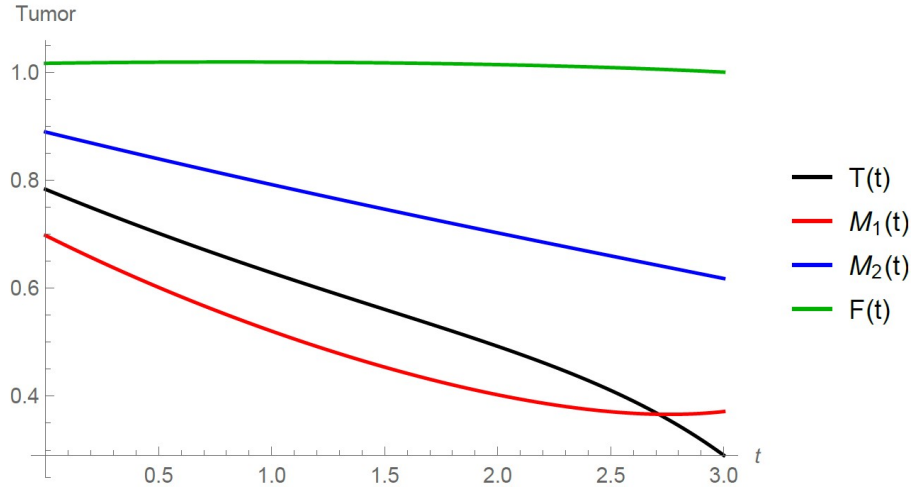

Figure 9. The ADM's solutions of System (3.3) at $\xi = \frac{1}{2}$.

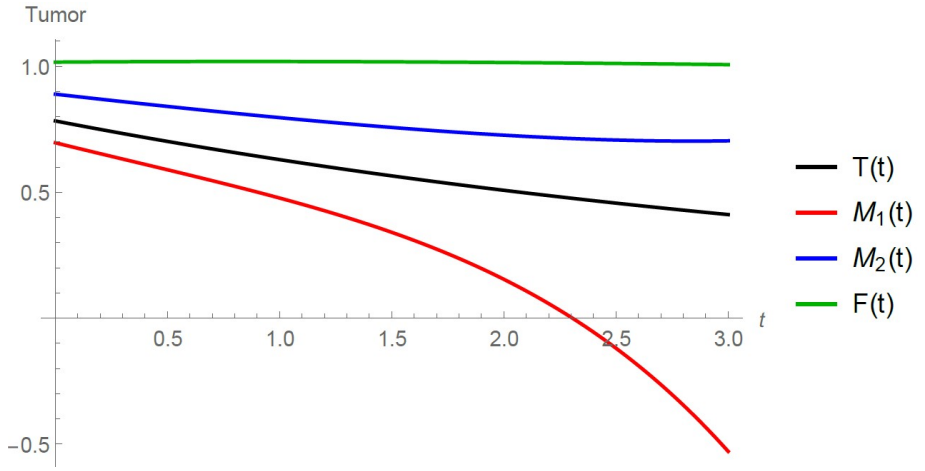

Figure 10. The PM's solutions of System (3.3) at $\xi = \frac{1}{2}$.

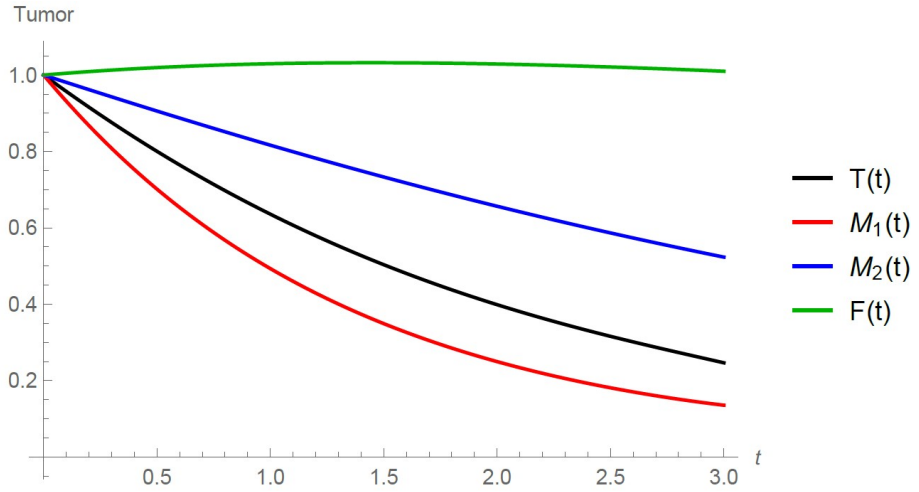

Figure 11. The ADM's solutions of System (3.3) at $\xi = 1$.

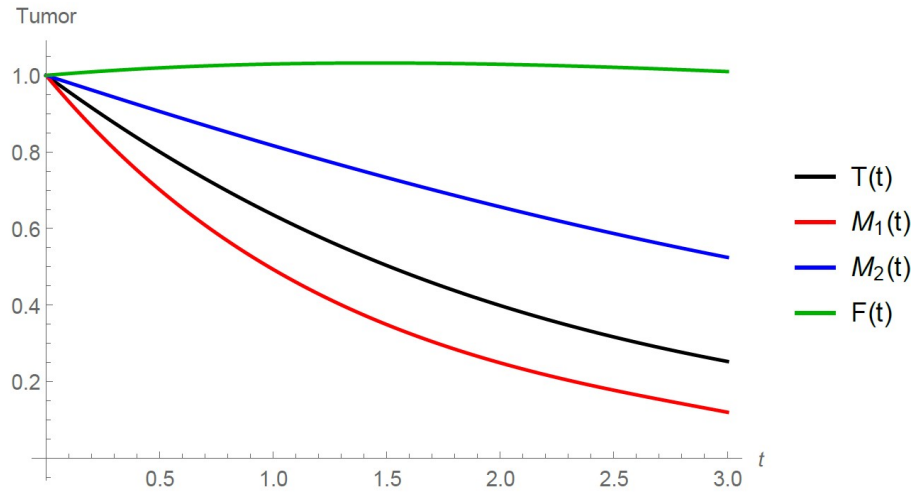

Figure 12. The PM's solutions of System (3.3) at $\xi = 1$.

8. Complex dynamics in the Tumor-macrophage interaction system (3.3)

In this section, System (3.3) is numerically integrated using the algorithm in [45] to show the existence of complex dynamics in the considered model. Throughout this section, the state variables (T, M_1, M_2, F) are replaced with (w, x, y, z), respectively. Parameter Set A

$$\begin{aligned} \alpha_1 &= 5,\ \alpha_2 = 2.5,\ \alpha_3 = 1,\ \beta_1 = 8.6,\ \beta_2 = 0.9,\ \beta_3 = 7.2,\ \gamma_1 = 9,\ \ \gamma_2 = 0.5,\ \delta_1 = 1, \\ \delta_2 &= 0.08,\ \mu_1 = 1,\ \mu_2 = 0.5,\ \mu_3 = 0.2,\ \mu_4 = 0.05,\ \mu_5 = 0.11, \end{aligned}$$

and the initial data $T(0) = 1.0006 \times 10^{-5}, M_1(0) = 1.0526 \times 10^{-5}, M_2(0) = 9.8612 \times 10^{-6}$, and $F(0) = 9.2871 \times 10^{-6}$ are used to produce Figure 13, in which a variety of complex dynamics are illustrated with numerous fractional parameter values ξ. Another set of parameters (Set B)

$$\alpha_1 = 7,\ \alpha_2 = 10,\ \alpha_3 = 0.9,\ \beta_1 = 8.6,\ \beta_2 = 0.9,\ \beta_3 = 10.2,\ \gamma_1 = 9,\ \ \gamma_2 = 0.5,\ \delta_1 = 1,$$

$\delta_2 = 0.085,\ \mu_1 = 1,\ \mu_2 = 0.5,\ \mu_3 = 0.2,\ \mu_4 = 0.05,\ \mu_5 = 0.2,$

and the initial data $T(0) = 1,\ M_1(0) = 1.2408,\ M_2(0) = 3.1415,$ and $F(0) = 3.6892$, are utilized to produce Figure 14, in which different roots of complex dynamics are demonstrated. In the last figure, a chaotic attractor is found when $\xi = 0.99$. A bifurcation diagram that explains the scenario of rich chaotic dynamics in this model is shown in Figure 15, which indicates that the pro-tumor cells $M_2(t)$ are completely unpredictable when the fractional-order ξ is close to 0.99. Moreover, the bifurcation diagram illustrated in Figure 16 indicates that the behavior of the feedback control variable $F(t)$ can not be predicted when the fractional-order ξ is increased toward 0.99.

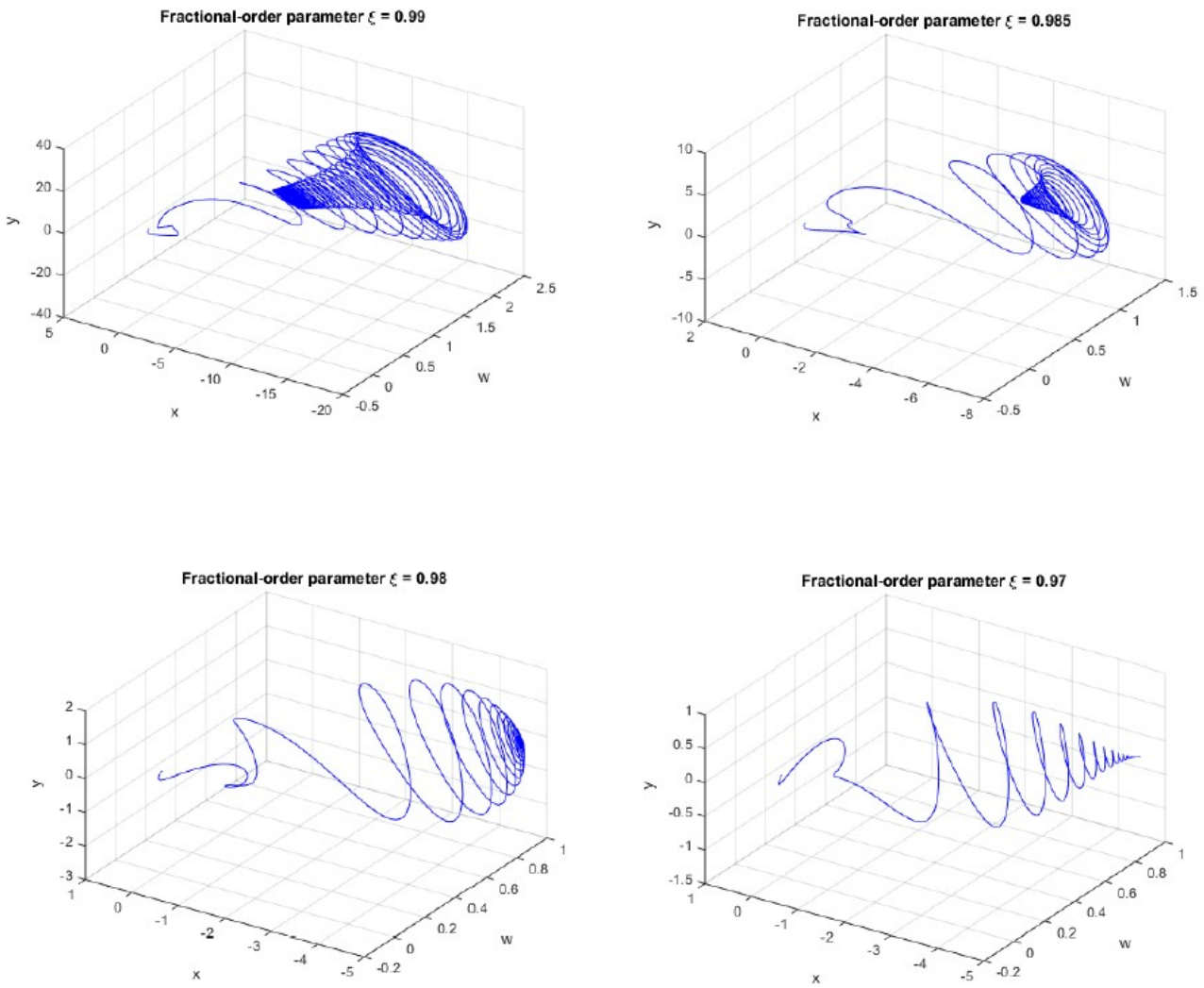

Figure 13. Phase diagrams of System (3.3) using parameter Set A and different values of ξ.

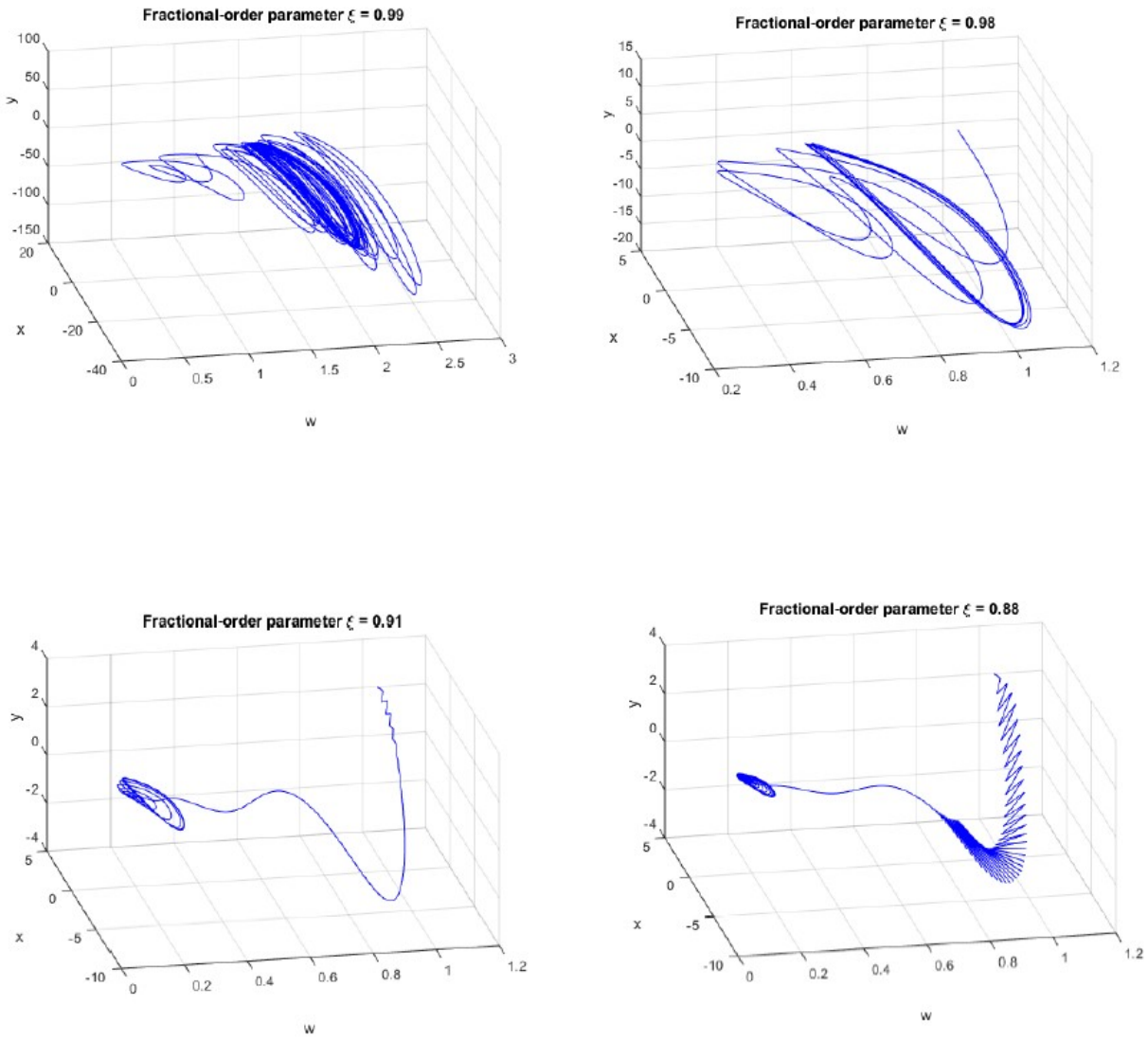

Figure 14. Phase diagrams of System (3.3) using parameter Set B and different values of ξ.

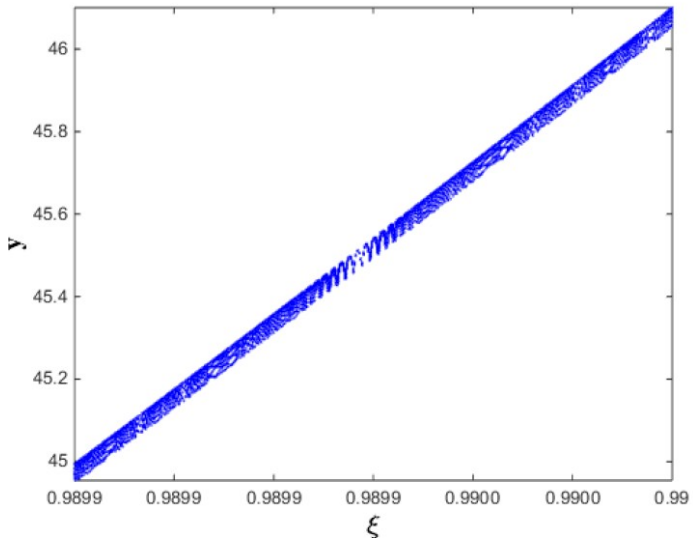

Figure 15. A bifurcation diagram of the pro-tumor cells $M_2(t)$ of System (3.3) as ξ is varied and using parameter Set B.

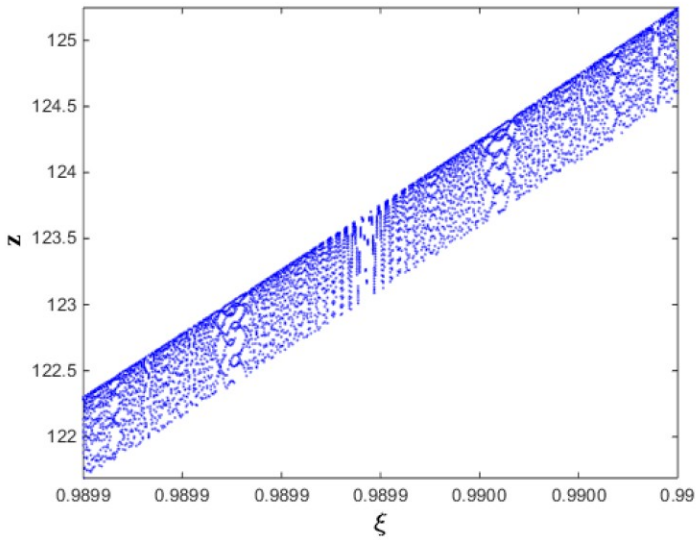

Figure 16. A bifurcation diagram of the feedback control variable $F(t)$ of System (3.3) as ξ is varied and using parameter Set B.

9. Conclusions

In this work, we developed and investigated a model of the interaction between tumors and macrophages that was controlled by the CF fractional derivative. The ADM was used to determine the uniqueness and convergence of the suggested model, and the PM was used to confirm the analytical results. The stability of tumor-free, tumor-dominant, and co-existence equilibria was thoroughly examined, and error estimation validated the ADM's dependability. Additionally, when the fractional

order becomes close to unity, numerical simulations demonstrated the existence of complicated dynamics, such as chaotic attractors and bifurcations. These results provide more realistic information on tumor immune interactions by highlighting the critical role fractional-order operators play in capturing memory effects and the hereditary features inherent in biological systems. In order to accurately reflect the tumor microenvironment, future studies could build on this work by adding more immune components and cytokine interactions, verifying the model using experimental or clinical data, and investigating spatial expansions using fractional partial differential equations. Further insights into treatment efficiency and the impact of various memory kernels on tumor-immune interactions may also be obtained by examining the best control strategies for therapy design and contrasting the CF derivative with other fractional operators, such as the Atangana-Baleanu operator.

Author contributions

Matouk: Conceived and designed the experiments; Performed the experiments; Analyzed and interpreted the data; Contributed reagents, materials, analysis tools or data; Wrote the paper. Ziada: Performed the experiments; Analyzed and interpreted the data; Contributed reagents, materials, analysis tools or data; Wrote the paper. Padder: Materials, analysis tools or data and wrote the paper. Botros: Performed the experiments; Analyzed and interpreted the data; Contributed reagents, materials, analysis tools or data; Wrote the paper. Hassan: Materials, analysis tools or data; Wrote the paper.

Use of Generative-AI tools declaration

The authors declare that they have not used Artificial Intelligence (AI) tools in the creation of this article.

Acknowledgments

The authors extend the appreciation to the Deanship of Postgraduate Studies and Scientific Research at Majmaah University for funding this research work through project number R-2026-193.

Conflict of interest

All authors declare no conflicts of interest in this paper.

References

1. M. R. Owen, J. A. Sherratt, Modelling the macrophage invasion of tumors: Effects on growth and composition, *IMA J. Math. Appl. Med.*, **15** (1998), 165–185. https://doi.org/10.1093/imammb/15.2.165
2. R. Eftimie, C. Barelle, Mathematical investigation of innate immune responses to Lung cancer: The role of macrophages with mixed phenotypes, *J. Theor. Biol.*, **524** (2021), 110739. https://doi.org/10.1016/j.jtbi.2021.110739

3. I. Podlubny, *Fractional differential equations*, 1999.
4. R. Hilfer, *Applications of fractional calculus in physics*, World Scientific Publishing Co. Pte. Ltd, 2000. https://doi.org/10.1142/3779
5. N. Laskin, Fractional market dynamics, *Physica A*, **287** (2000), 482–492. https://doi.org/10.1016/S0378-4371(00)00387-3
6. D. Baleanu, K. Diethelm, E. Scalas, J. J. Trujillo, *Fractional calculus: Models and numerical methods*, World Scientific, 2012.
7. A. Al-Khedhairi, A. E. Matouk, I. Khan, Chaotic dynamics and chaos control for the fractional-order geomagnetic field model, *Chaos Soliton. Fract.*, **128** (2019), 390–401. https://doi.org/10.1016/j.chaos.2019.07.019
8. A. E. Matouk, I. G. Ameen, Y. A. Gaber, Analyzing the dynamics of fractional spatio-temporal SEIR epidemic model, *AIMS Math.*, **9** (2024), 30838–30863. https://doi.org/10.3934/math.20241489
9. A. E. Matouk, *Advanced applications of fractional differential operators to science and technology*, 2020.
10. D. Baleanu, H. Mohammadi, S. Rezapour, A fractional differential equation model for the COVID-19 transmission by using the Caputo-Fabrizio derivative, *Adv. Differ. Equ.*, **2020** (2020), 299. https://doi.org/10.1186/s13662-020-02762-2
11. Z. Zhang, S. Jain, Mathematical model of Ebola and Covid-19 with fractional differential operators: Non-Markovian process and class for virus pathogen in the environment, *Chaos Soliton. Fract.*, **140** (2020), 110175. https://doi.org/10.1016/j.chaos.2020.110175
12. M. Caputo, Linear models of dissipation whose Q is almost frequency independent–II, *Geophys. J. Int.*, **13** (1967), 529–539. https://doi.org/10.1111/j.1365-246X.1967.tb02303.x
13. M. Caputo, M. Fabrizio, A new definition of fractional derivative without singular kernel, *Prog. Fract. Differ. Appl.*, **1** (2015), 73–85. https://doi.org/10.12785/pfda/010201
14. J. M. Cruz-Duarte, J. Rosales-Garcia, C. R. Correa-Cely, A. Garcia-Perez, J. G. Avina-Cervantes, A closed form expression for the Gaussian-based Caputo-Fabrizio fractional derivative for signal processing applications, *Commun. Nonlinear Sci.*, **61** (2018), 138–148. https://doi.org/10.1016/j.cnsns.2018.01.020
15. M. Ran, X. Liao, D. Lin, R. Yang, Analog realization of fractional-order capacitor and inductor via the Caputo-Fabrizio derivative, *J. Adv. Comput. Intell. Intell. Inform.*, **25** (2021), 291–300. https://doi.org/10.20965/jaciii.2021.p0291
16. A. M. Alqahtani, S. Sharma, A. Chaudhary, A. Sharma, Application of Caputo-Fabrizio derivative in circuit realization, *AIMS Math.*, **10** (2025), 2415–2443. https://doi.org/10.3934/math.2025113
17. D. Yu, X. Liao, Y. Wang, Modeling and analysis of Caputo-Fabrizio definition-based fractional-order boost converter with inductive loads, *Fractal Fract.*, **8** (2024), 81. https://doi.org/10.3390/fractalfract8020081
18. M. M. El-Dessoky, M. A. Khan, Application of Caputo-Fabrizio derivative to a cancer model with unknown parameters, *Discrete Cont. Dyn. S*, **14** (2020), 3557. https://doi.org/10.3934/dcdss.2020429

19. E. A. A. Ziada, M. Botros, Solution of a fractional mathematical model of brain metabolite variations in the circadian rhythm containing the Caputo-Fabrizio derivative, *J. Appl. Math. Comput.*, **71** (2025), 3353–3380. https://doi.org/10.1007/s12190-024-02327-6

20. Y. Chu, M. F. Khan, S. Ullah, S. A. A. Shah, M. Farooq, M. B. Mamat, Mathematical assessment of a fractional-order vector-host disease model with the Caputo-Fabrizio derivative, *Math. Method. Appl. Sci.*, **46** (2022), 232–247. https://doi.org/10.1002/mma.8507

21. M. A. Khan, Z. Hammouch, D. Baleanu, Modeling the dynamics of hepatitis E via the Caputo-Fabrizio derivative, *Math. Model. Nat. Phenom.*, **14** (2019), 311. https://doi.org/10.1051/mmnp/2018074

22. E. J. Moore, S. Sirisubtawee, S. Koonprasert, A Caputo-Fabrizio fractional differential equation model for HIV/AIDS with treatment compartment, *Adv. Differ. Equ.*, **2019** (2019), 200. https://doi.org/10.1186/s13662-019-2138-9

23. D. Baleanu, A. Jajarmi, H. Mohammadi, S. Rezapour, A new study on the mathematical modelling of human liver with Caputo-Fabrizio derivative, *Chaos Soliton. Fract.*, **134** (2020), 109705. https://doi.org/10.1016/j.chaos.2020.109705

24. O. J. Peter, Transmission dynamics of fractional order Brucellosis model using Caputo-Fabrizio operator, *Int. J. Differ. Equ.*, **2020** (2020), 2791380. https://doi.org/10.1155/2020/2791380

25. E. Bonyah, M. Juga, Fractional dynamics of coronavirus with comorbidity via Caputo-Fabrizio derivative, *Commun. Math. Biol. Neurosci.*, **2022** (2022), 12.

26. Z. Shah, N. Ullah, R. Jan, M. H. Alshehri, N. Vrinceanu, E. Antonescu, et al., Existence and sensitivity analysis of a Caputo-Fabrizio fractional order vector-borne disease model, *Eur. J. Pure Appl. Math.*, **18** (2025), 5687. https://doi.org/10.29020/nybg.ejpam.v18i2.5687

27. R. Shafqat, A. Alsaadi, Bifurcation in a fractional SIR model with normalized Caputo-Fabrizio derivative, *Discrete Dyn. Nat. Soc.*, **2025** (2025), 4368999. https://doi.org/10.1155/ddns/4368999

28. R. Shafqat, A. Al-Quran, A. Alsaadi, A. M. Djaouti, Normalized Caputo-Fabrizio SVIR modeling and bifurcation analysis, *Sci. Rep.*, **16** (2026), 8193. https://doi.org/10.1038/s41598-026-38301-4

29. T. Zhang, Y. Li, Global exponential stability of discrete-time almost automorphic Caputo-Fabrizio BAM fuzzy neural networks via exponential Euler technique, *Knowl. Based Syst.*, **246** (2022), 108675. https://doi.org/10.1016/j.knosys.2022.108675

30. A. E. Matouk, The impact of Caputo-Fabrizio operator on the complex dynamics of a multidrug resistance model, *AIMS Math.*, **11** (2026), 8655–8676. https://doi.org/10.3934/math.2026356

31. E. Ahmed, A. Hashish, F. A. Rihan, On fractional order cancer model, *J. Fract. Calc. Appl. Anal.*, **3** (2012), 1–6.

32. F. A. Rihan, A. Hashish, F. Al-Maskari, M. Sheek-Hussein, E. Ahmed, M. B. Riaz, et al., Dynamics of tumor-immune system with fractional-order, *J. Tumor Res.*, **2** (2016), 109–115. https://doi.org/10.35248/2684-1258.16.2.109

33. A. M. Wazwaz, A comparison between Adomian decomposition method and Taylor series method in the series solutions, *Appl. Math. Comput.*, **97** (1998), 37–44. https://doi.org/10.1016/S0096-3003(97)10127-8

34. A. Sadighi, D. D. Ganji, Exact solutions of Laplace equation by homotopy-perturbation and Adomian decomposition methods, *Phys. Lett. A*, **367** (2007), 83–87. https://doi.org/10.1016/j.physleta.2007.02.082

35. R. Rach, On the Adomian (decomposition) method and comparisons with Picard's method, *J. Math. Anal. Appl.*, **128** (1987), 480–483. https://doi.org/10.1016/0022-247X(87)90199-5

36. E. A. A. Ziada, H. Hashem, A. Al-Jaser, O. Moaaz, M. Botros, Numerical and analytical approach to the Chandrasekhar quadratic functional integral equation using Picard and Adomian decomposition methods, *Electron. Res. Arch.*, **32** (2024), 5943–5965. https://doi.org/10.3934/era.2024275

37. E. A. A. Ziada, M. Botros, Solution of a fractional mathematical model of brain metabolite variations in the circadian rhythm containing the Caputo-Fabrizio derivative, *J. Appl. Math. Comput.*, **71** (2025), 3353–3380. https://doi.org/10.1007/s12190-024-02327-6

38. E. A. A. Ziada, S. El-Morsy, O. Moaaz, S. S. Askar, A. M. Alshamrani, M. Botros, Solution of the SIR epidemic model of arbitrary orders containing Caputo-Fabrizio, Atangana-Baleanu and Caputo derivatives, *AIMS Math.*, **9** (2024), 18324–18355. https://doi.org/10.3934/math.2024894

39. L. Wang, A new algorithm for solving classical Blasius equation, *Appl. Math. Comput.*, **157** (2004), 1–9. https://doi.org/10.1016/j.amc.2003.06.011

40. S. Momani, Z. Odibat, Analytical solution of a time-fractional Navier–Stokes equation by Adomian decomposition method, *Appl. Math. Comput.*, **177** (2006), 488–494. https://doi.org/10.1016/j.amc.2005.11.025

41. G. A. M. Nchama, L. D. Lau-Alfonso, A. M. L. Mecias, M. R. Ricard, Properties of the Caputo-Fabrizio fractional derivative, *Appl. Math. Inf. Sci.*, **14** (2020), 761–769. https://doi.org/10.18576/amis/140503

42. H. Li, J. Cheng, H. B. Li, S. M. Zhong, Stability analysis of a fractional-order linear system described by the Caputo-Fabrizio derivative, *Mathematics*, **7** (2019), 200. https://doi.org/10.3390/math7020200

43. Y. Shu, J. Huang, Y. Dong, Y. Takeuchi, Mathematical modeling and bifurcation analysis of pro- and anti-tumor macrophages, *Appl. Math. Model.*, **88** (2020), 758–773. https://doi.org/10.1016/j.apm.2020.06.042

44. A. E. Matouk, Fractional Routh-Hurwitz conditions and nonlinear dynamics in some 3D and 4D dynamical systems modeled by Caputo-Fabrizio operators, *Results Appl. Math.*, **26** (2025), 100588. https://doi.org/10.1016/j.rinam.2025.100588

45. A. E. Matouk, M. Botros, Hidden chaotic attractors and self-excited chaotic attractors in a novel circuit system via Grünwald-Letnikov, Caputo-Fabrizio and Atangana-Baleanu fractional operators, *Alex. Eng. J.*, **116** (2025), 525–534. https://doi.org/10.1016/j.aej.2024.12.064